East Anglia THREE

Appendix 9.1
Underwater Noise Modelling

This Page Is Intentionally Blank

Table of Contents

9 UNDERWATER NOISE MODELLING

9.1 Introduction

1. This report estimates the underwater acoustic emissions associated with construction, operation and decommissioning at the East Anglia THREE site and assesses the potential for the pile driving noise to impact marine fauna. The National Physical Laboratory (NPL) has been contracted by East Anglia THREE Limited (EATL) to undertake an assessment of underwater noise from piling, to inform the Environmental Statement for the proposed East Anglia THREE project. The modelling methodology for this assessment is described in detail in Section 9.3, and is designed to estimate the likely underwater noise levels generated by construction at the East Anglia THREE site in order to inform of the potential radiated underwater noise levels, to be used in the marine mammal (Chapter 12 Marine Mammal Ecology) and fish assessments (Chapter 11 Fish and Shellfish Ecology). Consideration was also given to the potential for auditory injury from prolonged exposure and the effect of multiple concurrently operating piling vessels.

2. The assessment was undertaken in the context of guidance documents and directives relating to underwater noise (JNCC 2010; NPS EN-1 July 2011; NPS EN- 3 July 2011; MSFD 2008/56/EC 2008; Robinson et al. 2014).

3. Consideration of the worst case sound source is based on the use of impact pile-driving. It is expected that the wind turbine foundations would be driven by hammers with a rated energy of up to 3,500kJ. The full hammer energy may not be used for every piling sequence or at the onset of piling. However, it may be required to install foundations to full design penetration, depending on the final pile length, geometry, diameter, soil strength and composition at each location. The underwater sound propagation modelling for the East Anglia THREE site was undertaken assuming a 3,500kJ hammer strike energy, as well as, a number of smaller hammer strike energies including 1,400kJ, 2,000kJ, 2,300kJ and 3,000kJ to account for the fact that the maximum rated hammer energy may not be required for all locations, and would not be expected to be employed during the whole piling sequence. In terms of assessing the impact of underwater noise, the impact would be receptor driven and is assessed in Chapter 11 Fish and Shellfish Ecology, and Chapter 12 Marine Mammal Ecology.

9.2 Introduction to Underwater Acoustics

9.2.1 Basic Acoustic Concepts

4. This section outlines some of the relevant concepts in underwater acoustics to help the non-specialist reader to best understand the assessment presented in this report.

5. Underwater sound can be described as a pressure wave travelling through the water, which can travel much greater distances than sound in air. It is the low absorption in water (Kinsler et al. 1982; Kaye and Laby 2004) that allows sound to travel large distances in the ocean, particularly low frequency sound.

6. An important characteristic of sound is its frequency, described as the number of oscillations per second, the unit of frequency being the hertz (Hz). Measured observations describing impact piling show that most of the sound energy is present between frequencies of around 100 and 400Hz. When displaying the measured values, it is common to see the frequency range divided up into one-third octave bands (TOB) which help express the sound level as a function of frequency, where each band represents one-third of an octave, an octave representing a doubling of frequency.

7. The amplitude of the sound can be described in terms of the sound pressure where the unit of pressure is the pascal (Pa) or newton per square metre (Nm^{-2}). However, by convention sound levels are expressed in decibels (dB) relative to a reference pressure, which is 1 µPa for underwater sound. Metrics most commonly used to describe the underwater sound in impact piling in the UK include peak-to-peak pressure level and Sound Exposure Level (SEL). It is common to see peak and peak-to-peak pressure levels reported, where for a symmetric pulse waveform, the peak-to-peak pressure level will be twice the value of the peak pressure level (a difference of 6dB). Sound Pressure Level (SPL) is another common metric in underwater acoustics and, by convention, is expressed as a root mean square (RMS) value. SPL is most useful to describe the level of a continuous type noise such as shipping or operational turbine noise. More detailed descriptions and meanings of the metrics can be found in the *Good Practice Guide for Underwater Noise Measurement* (Robinson et al. 2014). Further details can also be found in Annex A.

8. Source Level (SL) is a metric used in underwater acoustics to describe the source output amplitude. The decibel units for this quantity may be written as dB re 1 µPa·m, however, the unit is more commonly seen expressed as dB re 1 µPa at 1m. It should be noted that source level is an idealised acoustic far-field parameter and is by definition a derived quantity and not a measurement at a distance of 1 metre from the source.

9.   Propagation Loss (PL) or Transmission Loss (TL) is the term used to describe the reduction of the sound level as a function of distance from an acoustic source. The mechanisms by which the sound intensity reduces are primarily geometrical spreading, sound absorption in the water and losses into the sea bed or scattering from other boundaries. In shallow water, particularly with varying bathymetry, this can be quite complicated due to multiple interactions with the surface and sea bed. The depth can also restrict the propagation of lower frequencies in shallow water. It is normal for PL (or TL) to be stated as a positive number in dB representing the loss for the total range between the reference distance (1m for SL) and the receiver location. The quantity is a function of frequency, and depends, for example, on sea bed type, bathymetry, surface roughness, sound speed profile.

10.   The Received Level (RL) is the acoustic pressure, expressed as a level, measured by a hydrophone at some distance away from a sound source. It is also considered to be the sound pressure which arrives at any acoustic receptor which is exposed to a sound. The received level might be expressed in a number of ways, for example as a SPL (dB re 1 µPa) or a SEL (dB re 1 µPa^2·s). When predicting received level from estimated source level for zones of impact, the received level is simply determined by subtracting the PL in dB from the SL in dB, RL = SL − PL, where the PL is estimated using a PL model (more information on numerical propagation models is given in Section 9.3 and Annex A). When the SL is estimated from a measured RL then the SL is simply found by addition of RL and PL, SL = RL + PL. To calculate transmission loss accurately requires an accurate model for the propagation of the sound and its interaction with the sea bed and sea surface.

11.   An important point to note is that the source level for marine piling reported in previous windfarm studies have often been obtained by extrapolation back to the origin of the source using simple spreading formulae that approximate the transmission loss from measured data (data fits). As such, these reported values are not true source levels and are generally not consistent with the accepted definition of source level by Urick (1983) and Ainslie (2011), including the draft ISO standard 'Underwater acoustical terminology' (ISO/TC43/SC3/WG2). To distinguish between formats, data derived from simple spreading formulae (empirical data fits) are sometimes referred to as "Effective SL'', and are not suitable for use in numerical propagation models. Care should be taken when comparing published source level values.

12.   Typically, the characteristics of an acoustic pulse propagating in shallow water do not only depend on the distance from the source. The transmission may show a strong dependence on frequency due to the modal nature of the propagation in the shallow-

water channel and the frequency-dependent absorption in the water and in the sediment.

13. Ambient noise originates from a range of noise sources, both natural and anthropogenic and spans a large frequency range from below 1Hz, to well over 100kHz. It is most commonly expressed as power spectral density levels in TOB in units of dB re 1 µPa2Hz-1, where the values have been divided by the bandwidth of each TOB. This is different from TOB power spectra (dB re 1 µPa²) which are more appropriate for radiated noise, where the total energy or power in the signal is of interest. In general, ambient noise measurements in the UK coastal waters indicate that maximum TOB power spectral noise density levels are typically between around 95 and 120dB re 1 µPa²Hz⁻¹ with these peak band levels generally occurring between frequencies of a few tens of hertz to a few hundred hertz, depending on location and time (Nedwell et al. 2007; Theobald et al. 2010; Robinson et al. 2011).

14. A number of sounds with various characteristics have been associated with the construction, operation and decommissioning of offshore windfarm developments. Noise from piling during the construction phase will be the prevalent source and this entails driving a wind turbine foundation into the sea bed using an impact hammer and usually involves a gradual ramp-up in hammer energy (soft-start) until the maximum applied hammer strike energy is reached, which may then continue for several hours. Underwater noise from impact piling is known to generate considerably high peak pressure levels and SEL values and may be expected to be distinguishable above ambient noise over distances of several tens of km from the source (Thomsen et al. 2006; Nedwell et al. 2007; Bailey et al. 2010). The noise levels that would be propagated depend on a number of factors which include the foundation type, the installation method, and noise propagation conditions in the area. Other sounds sources would also be present that would be lower in sound level, but may be present for extended periods of time. Examples include surface vessel noise and noise radiated from operational wind turbines.

9.3 Underwater Noise Propagation Modelling

9.3.1 Noise Propagation Model

15. The underwater sound propagation modelling employed for this study has been undertaken by NPL. Potential impact ranges from pile driving have been estimated using an energy flux solution proposed by Weston (1976), which is capable of propagation over large distances whilst accounting for range-dependent bathymetry. The Weston energy flux underwater sound numerical propagation model has been implemented;

- with the frequency-dependent absorption formula from Thorpe (1967);

- including the effect of surface scattering (Coates 1988; Medwin and Clay 1998; Ainslie et al. 1994);

- using common sediment acoustics properties across the modelled area, which are representative of those expected to result in greater propagation distances (Hamilton 1980; Lurton 2003); and

- using GEBCO Digital Atlas bathymetry data over an area extending approximately 100km around the windfarm boundary, augmented with higher resolution bathymetry data, where available (both lowest and highest astronomical tides are considered to ensure the longest propagation ranges are captured).

16. For shorter range modelling, for the purpose of establishing injury ranges following criteria specified in Chapter 12 Marine Mammal Ecology for marine mammals and Chapter 11 Fish and Shellfish Ecology for fish, a higher data resolution was used. The Weston energy-flux model assumes a homogenous sound speed profile which is often the case in coastal waters due to tidal mixing. The Weston energy-flux model has been benchmarked, with good agreement, against other transmission loss models published in the literature including the Range-dependent Acoustic Model (RAM) implementation of the parabolic equation (PE) solution (Collins 1993) based on AcTUP V2.2L (Maggi and Duncan 2010), an image source model (Urick 1983), a wavenumber integration transmission loss model (OASES), and a normal mode model (Kraken) and against measurement data. Benchmarking of these models is detailed in Wang et al. (2014) and validation of the Weston energy-flux model against measurement data is discussed in Annex B.

17. The energy flux propagation model has been used to propagate an SEL source level to establish the SEL received level as a function of range. To derive a source level for use in the model, a monopile SEL source level was specified in TOB using a spectral source level shape taken from Ainslie et al. (2012) and scaled using a broadband SEL source level calculated by De Jong and Ainslie (2008) from piling measurement data published in Robinson et al. (2007) for a UK windfarm. The SEL source level or acoustic pulse energy source level has been assumed to scale up linearly with hammer energy as demonstrated by measurements during a full piling sequence, including the piling soft-start, by Robinson et al. (2007 and 2009b). This scaling was applied using a theoretical maximum scaling of SEL, directly with the hammer energy i.e., a doubling of hammer energy results in a 3dB increase in acoustic energy expressed in dB units (SEL). The dimensions of the pile are not expected to have a significant effect on the radiated noise energy if the hammer energy remains the same (Nehls et al. 2007).

Based on the available information (Robinson et al. 2007 and 2009b, and Nehls et al. 2007), the source level is therefore scaled by hammer energy regardless of the pile size.

18.   The received levels for each TOB are obtained from the difference between the source level and the propagation loss in each TOB (see Section 9.2 and Annex A), which can be summed up to obtain the broadband or pulse SEL for the given bandwidth.

19.   The peak pressure level of the sound pulse generated by the impact piling can decay at a slightly higher rate compared to the energy in the pulse (the SEL is proportional to pulse energy) due to temporal dilation of the pulse that results from multiple reflections from the sea bed and the sea surface as the sound pulse propagates. To allow the peak pressure level to be propagated as a function of range, an extra loss term was applied to the energy flux model to account for this more rapid peak pressure level decay. This loss term was established using the OASES wavenumber integration transmission loss model by estimating the difference in transmission loss between the pulse energy and the peak pulse pressure for a single flat bathymetry transect for various water depths and was validated against previous underwater noise measurement data from impact piling of the peak pressure level and pulse SEL metrics. For the propagation of peak pressure level, a scaling factor was applied to convert the pulse energy source level to a peak pressure source which was based on measurement data where sound exposure level of the pulse and peak pressure data were measured at ranges of 750m and less to the pile, and where the hammers were operating in the upper range of their rated hammer energy (i.e., where the hammer has the shortest impact time on the anvil or pile).

9.3.2   Modelled Sound Propagation for Single Pile Locations to Estimate Potential Impact Ranges

20.   Underwater sound propagation was modelled at twenty locations within the East Anglia THREE site with the aim of estimating the potential impact ranges. The locations were selected to encompass a range of sound propagation conditions resulting from variation in bathymetry, including locations near up-sloping and down-sloping profiles, in addition to covering the geometrical extent of the East Anglia THREE site. The location details are provided in Annex C of this report. The modelled hammer energies are summarised in Table 9.1.

21.   For each modelled position within the East Anglia THREE site, a sound propagation map was obtained showing the noise level as a two-dimensional function of range.

22.   At short ranges from the pile (few km), the broadband underwater sound propagation generally appears symmetrical (i.e., similar irrespective of the bearing from the pile).

This is due to relatively small variation in the propagation environment over shorter distances compared with the variation over greater distances.

23. The image in Plate 9.1 shows a propagation modelling output representative of the acoustic field around the mid-water column at an example location within the East Anglia THREE site for a hammer strike energy of 3,500kJ.

24. In addition to modelling the average received level representative of levels around the mid-water column, the received level variation through the water column was modelled as described in Section 9.3.5 for an example location and results of this are presented in Plate 9.2. There is substantial variation expected through the water column with the pressure levels reducing near the sea bed due to interactions with sea bed and near the surface due to the pressure release nature of the water / air boundary.

25. There is considerable variability in the sound propagation due to variable bathymetry across and beyond the East Anglia THREE site. In general, the noise propagates efficiently over down-sloping sea bed, which in places, is followed by shallower channels along a given transect, confining the sound energy. This effect particularly occurs to the south-west, west and north-west. There is also a strong influence from long sand banks in the area, which results in asymmetric propagation as seen in Plate 9.1.

26. Generally, for the conditions around the East Anglia THREE site, shallower water, at the pile location, will result in slightly higher received level close to the source when compared with deeper water locations, due to the sound energy being trapped in a smaller water volume. For the propagation conditions around the East Anglia THREE site, at ranges greater than around 10km, this effect is overcome by the interactions of the propagating sound with the boundaries, manifested as loss of the sound energy. This may also lead to slight variations in propagation efficiency due to tidal variation, although this has a relatively small effect for the East Anglia THREE site because of a small tidal variation to water depth ratio. However, small differences may be expected to occur with the highest sound levels expected at shorter ranges during lowest astronomical tide and highest sound levels at large ranges (> about 10km) during highest astronomical tide. For this reason, the distances over which injury and behavioural disturbance might be expected were obtained for both LAT and HAT and the longer of the two reported in each case.
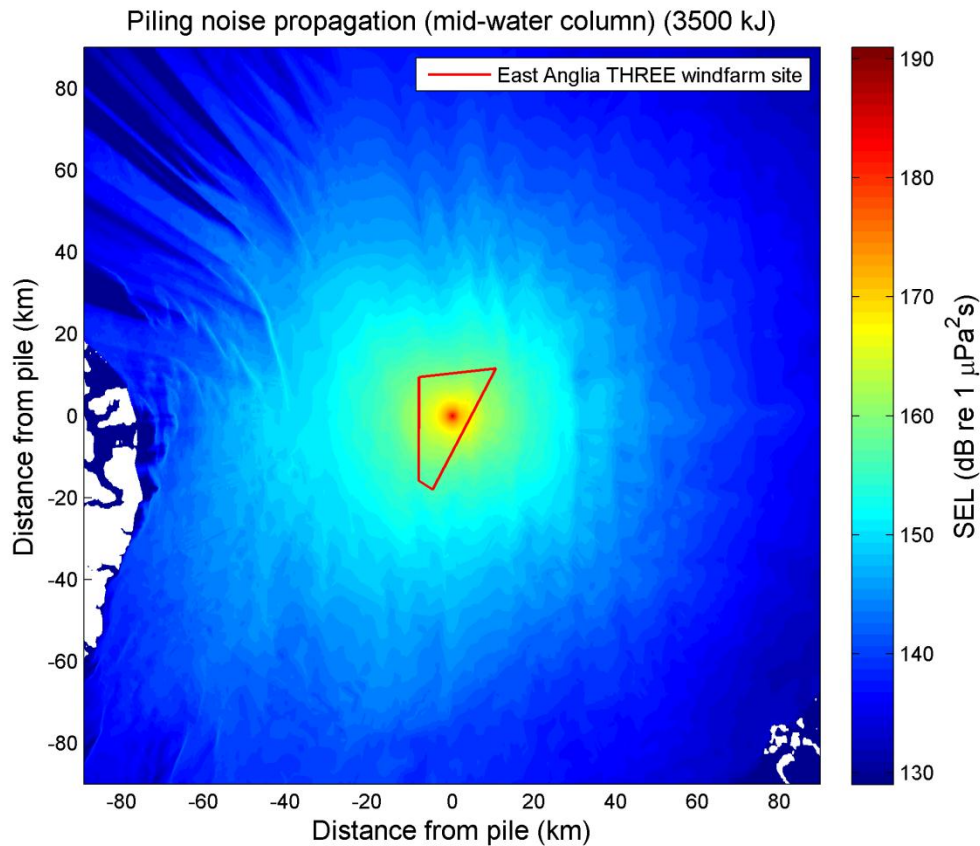
Plate 9.1. Impact piling noise propagation output for a single pile example location (Location ID17, Annex C, Table 9.13) modelled within East Anglia THREE for a 3,500kJ hammer strike energy.

9.3.3   Modelling the Windfarm Construction Noise Footprint

27.   Impact piling is a transient activity which is only likely to occur concurrently at a small number of locations within a windfarm project, where the exact locations at any given time and timing of the construction activities are unknown. To illustrate the total spatial extent of the potential impact ranges resulting from the underwater noise during the construction phase, the sound propagation was modelled at various locations (twelve in total) along the East Anglia THREE site boundary (location details are provided in Annex C of this report), resulting in a noise footprint. The noise footprint can be considered to show the possible impact ranges for a given threshold which might occur, around the boundary of the windfarm, irrespective of the timing, specific location or number of piling vessels operating within the project boundary. Examples of the construction noise footprints are illustrated in Plate 9.5 and Plate 9.11 for harbour porpoise *Phocoena phocoena* and fish, respectively.

9.3.4 Modelling the Effect of Multiple Piling Vessels

28.   The use of multiple piling vessels, considered for the foundation installation at the East Anglia THREE site, could potentially increase the area of the sea where the noise from piling is present at levels which might result in an impact. The area effected during concurrent piling would depend on the separation distance between piling vessels (i.e. whether the impact zones from each vessel overlap or not). An illustrative scenario has been modelled with two piling vessels with different separation distances.   As it is highly unlikely that the sound pulses would interfere constructively, the sound levels would not be expected to increase as a result of summation. The results of this multiple piling vessel modelling are presented and discussed further in Section 9.4.1.3.

9.3.5 Modelling Sound Pressure as a Function of Position in the Water Column

29.   For the propagation conditions around the East Anglia THREE site, the broadband noise levels at larger ranges from the source (greater than around 1km from the source) resulting from impact piling are expected to be lower near the sea bed than they are around mid-water depth. Due to the pressure release effect of the surface, the noise levels towards the water surface would also be much lower than deeper down around the mid-water column.

30.   The energy flux model described in Section 9.3.1 only considers the sound energy propagating through the water column and so does not provide vertical profile data. As described above, this would not be the case in reality, where it would be expected that the broadband sound pressure would be reduced near the surface and the sea bed. This is important when considering the potential impact of underwater noise on sea bed dwelling species and species near the surface.

31.   To investigate this effect a more comprehensive propagation model (computationally more intensive) was used in addition to the energy flux model. Underwater sound propagation was modelled along two transects over a distance of around 50km, radiating northward and southward from an example pile location in the East Anglia THREE site. This example location and respective transects were chosen as they allow demonstration of sound propagation along both, up- and down-sloping environments.

32.   The model used was the AcTUP V2.2L version of RAM (Collins 1993), a PE model (described in Annex A), with the actual implementation based on RAMGeo. This is one of the most widely used ocean acoustic propagation models and has been benchmarked alongside other acoustic propagation models, including the Weston (1976) energy flux mode, by Wang et al. 2014.

33. The results of the RAM modelling are shown in Plate 9.2 for the two transects diverging from the pile using the same environmental properties outlined in Section 9.3.1. The modelling shows two important points:

- The broadband noise level, as a result of complex interaction of the sound wave with the sea bed, can be several dB lower near the sea bed compared to around mid-water column at ranges exceeding the first few km. The effect is potentially weakest where the sea bed is rapidly up-sloping. The implication of this is that animals, which dwell on or near the sea bed, such as some fish for example (e.g. demersal fish), would be exposed to sound pressures that are potentially lower than those predicted in the energy flux model described in Section 9.3.1. However, these are broadband levels and this generalisation would not be true at all frequencies. This model does also not account for the vibration travelling along the sea bed, which may generate a surface wave in the sediment with a velocity or displacement component to which fish may be sensitive (Hawkins 2009). Whilst sound originating from the section of the pile below the sea bed would generally attenuate more rapidly that in the water, the surface wave travelling along the surface of the sea bed may generate particle velocity components to which fish would likely be sensitive (Hawkins 2009; Hazelwood 2012).

- The noise level close to the sea surface is tens of dB lower compared to the mid-water noise levels at relatively short distances from the pile. This would result in a reduced exposure of any animal travelling at the surface which would likely reduce the area of avoidance from the pile. It would also result in a substantially reduced SEL dose (further described in Section 9.3.6) for any animal which might swim away, from the sound source at shallow depth (i.e. near the surface).

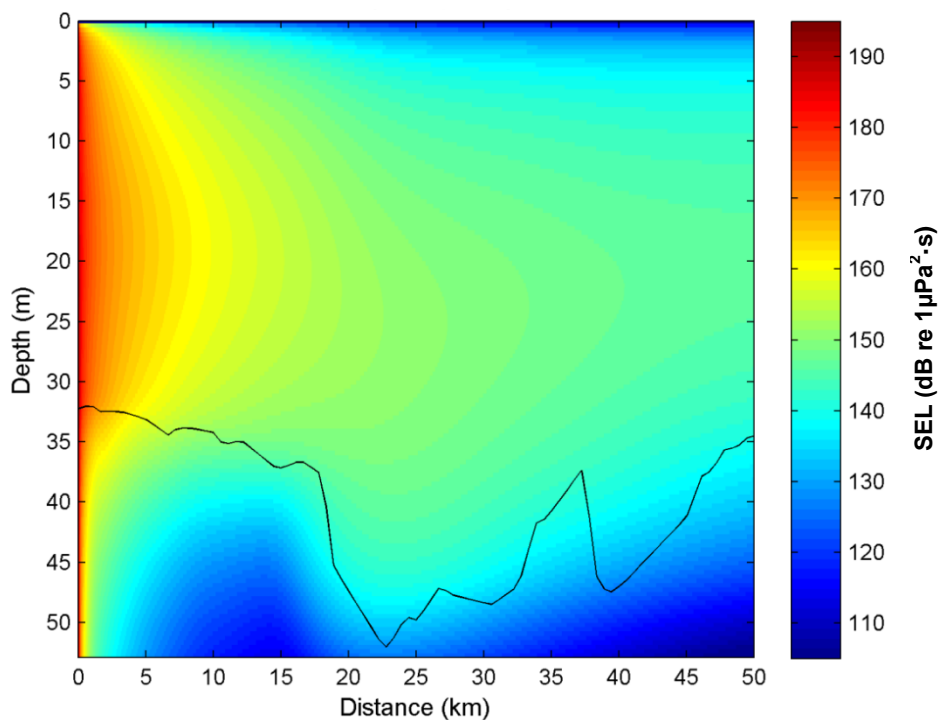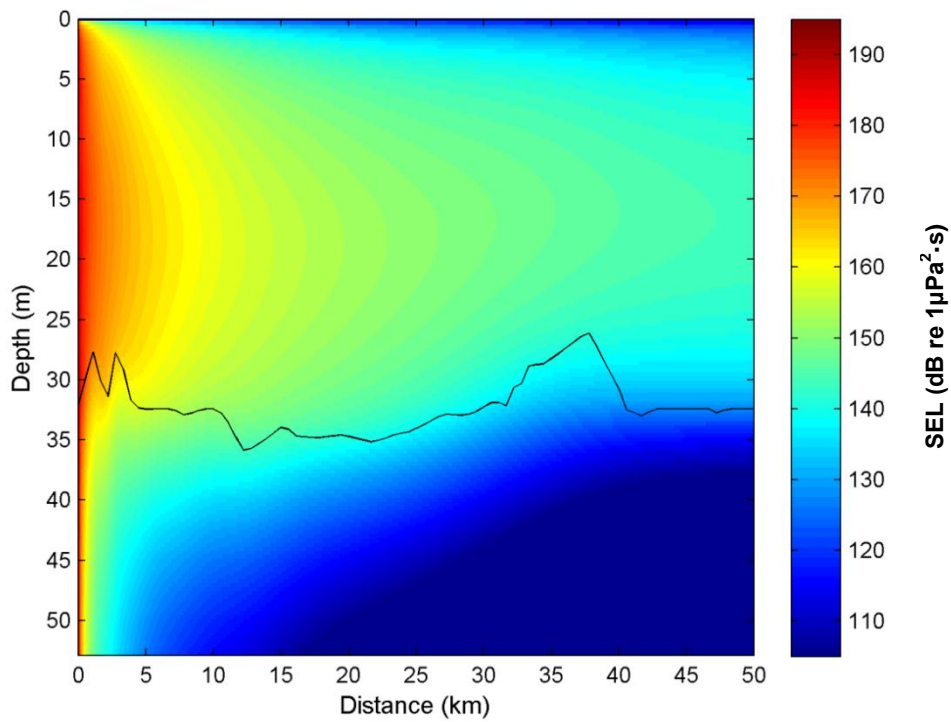**Plate 9.2. Propagation, as a function of depth and range (shown as broadband SEL dB re 1 μPa²·s), along two ~50km long transects radiating northward (top panel) and southward (bottom panel), from a pile location within East Anglia THREE (Location ID17, see Annex C, Table 9.9). Bathymetric profile is indicated with a black line.**

9.3.6 Sound Exposure Level (SEL) Dose Modelling

34. The effect of continued exposure during a piling sequence (i.e., exposure to more than one sound pulse) has the potential to result in the onset of PTS at ranges greater than those for auditory injury from a single pulse (i.e., instantaneous auditory injury). This results from the combined effect of a sequence of piling pulses, which can be summed up as sound energy to provide the SEL dose (Theobald et al. 2009; Lepper et al. 2011). This is analogous to how noise exposure is assessed for humans, which considers exposure to noise over a working day in accordance with the Control of Noise at Work Regulations 2004.

35. To illustrate the potential for the onset of PTS from prolonged exposure to marine mammals, the SEL dose was modelled for an example piling sequence and is presented in Section 9.4.1.1.2.

9.3.7 Summary of Underwater Noise Modelling Carried Out for the East Anglia THREE site

Table 9.1. Summary of Underwater Noise Modelling Carried Out for the East Anglia THREE site.

Brief description	Purpose	Modelling details
Modelled sound propagation for single pile locations to estimate potential impact ranges, relating to sound pressure	Modelling of impact piling for 20 foundation locations to establish instantaneous injury and avoidance ranges for both LAT and HAT	• Weston (1976) energy flux model used. • Range of hammer energies modelled: 1,400kJ; 2,000kJ; 2,300kJ; 3,000kJ; 3,500kJ. • Injury or behavioural disturbance ranges for specified criteria (maximum was taken from LAT and HAT).
Modelling the windfarm construction noise footprint, relating to sound pressure	Modelling of 12 locations along the East Anglia THREE site boundary to establish the noise footprint to show noise resulting from construction irrespective of the timing, specific piling location or number of piling vessels operating within the project boundary	• Weston (1976) energy flux model used. • Range of hammer energies modelled: 1,400kJ; 2,000kJ; 2,300kJ; 3,000kJ; 3,500kJ.
Modelling the effect of multiple piling vessels, relating to sound pressure	Illustrative modelling of two concurrent piling vessels operating with two different separation distances	• Weston (1976) energy flux model used. • Hammer energy of 3,500kJ. • Vessel separations of ~4km and ~33km.

Brief description	Purpose	Modelling details
Modelling sound pressure as a function of position in the water column	To investigate variation of sound pressure to which animals might be exposure when at different depths.	• AcTUP V2.2L – RAMGeo model used. • Range of hammer energies modelled: 1,400kJ; 2,000kJ; 2,300kJ; 3,000kJ; 3,500kJ. • Two transects modelled (northward and southward) to represent up- and down-sloping environments.
Sound Exposure Level (SEL) dose modelling	Illustrative modelling of Sound Exposure Level (SEL) dose carried out for single location to assess potential for prolonged exposure to result in PTS	• Weston (1976) energy flux model used. • Hammer energy ramp up from 1,400kJ to 3,500kJ for a piling duration of 230 minutes. • Location with greater propagation ranges modelled. • Minimum 500 m start distance assumed at the onset of piling. • Animal assumed to swim away at onset of piling. • Animal assumed to remain submerged at a water depth where highest levels generally occur for the duration of piling. • No inter-pulse hearing recovery assumed. • No effective quiet hearing recovery assumed.

9.4 Estimated Injury and Avoidance Ranges Resulting from Underwater Noise for the East Anglia THREE site

9.4.1 Construction Phase

36. Underwater noise from impact piling is known to result in significant peak pressure levels and SEL and will be distinguishable above ambient noise over distances of several tens of km from the source (Thomsen et al. 2006; Nedwell et al. 2007; Bailey et al. 2010). Foundation types which rely on impact piling are considered the worst case in terms of the resulting underwater noise and other foundation types are therefore not considered in this aspect of the assessment.

37. Using the modelled noise levels presented in Section 9.3 and the impact criteria for marine mammals and fish specified in Chapter 12 Marine Mammal Ecology and Chapter 11 Fish and Shellfish Ecology, respectively, it is possible to establish ranges or zones over which marine mammals and fish might be impacted during the

construction phase of the proposed East Anglia THREE project. This is based on the effects of marine impact piling, the most prevalent high amplitude underwater noise source associated with the construction of a windfarm.

38. As discussed in Section 9.3, a range of hammer blow energies were considered to represent the range of sound levels that may be experienced at the East Anglia THREE site.

39. Noise would also result from vessels used during the construction of the windfarm. However, noise levels reported by Malme et al. (1989) and Richardson et al. (1995) for large surface vessels indicate that physiological damage to marine fauna is unlikely, although the levels could be sufficient to cause local disturbance of sensitive marine fauna in the immediate vicinity of the vessel, depending on ambient noise levels.

9.4.1.1   Marine Mammals

9.4.1.1.1   Onset of Auditory Injury (PTS Onset)
40. Potential ranges for the onset of instantaneous auditory injury for marine mammals during impact piling at the East Anglia THREE site are indicated in Tables 9.2**Error! eference source not found.** to 9.5 below**Error! Reference source not found.**, based on the injury criteria specified in Chapter 12 Marine Mammal Ecology.

41. The predicted noise levels in close proximity to the pile are comparable to those estimated for the onset of auditory injury and mortality would only be expected at noise levels substantially above those necessary to cause auditory injury. The pile driving installation is thus unlikely to result in radiated noise levels sufficient to cause instantaneous mortality in marine mammals beyond a few metres from the pile (Richardson et al. 1995 (converted from Yelverton et al. (1975) for marine mammals).

9.4.1.1.2   Prolonged Exposure (SEL Dose)
42. As outlined in Section 9.3.6, illustrative modelling of Sound Exposure Level (SEL) dose was carried out for a single location.

43. The SEL dose has been modelled for the following four functional hearing groups defined by Southall et al. (2007): (i) High-frequency cetaceans ; (ii) Mid-frequency cetaceans ; (iii) Low-frequency cetaceans; and Pinnipeds (in water). The modelling considers the SEL dose received from a single pile installation.

44. The piling sequence was based on the use of a 3,500 kJ strike energy as the full hammer energy. A 20 minute soft-start period was assumed to start at 20% of the full hammer energy and was gradually stepped up to full hammer strike energy at a

constant strike rate, with a total piling duration of 230 minutes. The piling sequence that was considered in the modelling is further detailed in Annex D.

45. The modelling was carried out for a location and transect with modelled transmission losses representative of some of the longer modelled propagation ranges for the East Anglia THREE site.

46. The SEL dose has been estimated by summing up the SEL received levels, for each pile strike, for the entire piling sequence, assuming a fleeing animal which moves away from the source once piling starts and continues to move away, around mid-water column, throughout the piling sequence. The adopted swim speed was 1.5 ms^{-1} for all species (based on data from Otani et al. 2000; Culik et al. 2001; Akamatsu et al. 2007), with the exception of baleen whales, where a swim speed of 3.25 ms^{-1} was adopted, based on published values for minke whale *Balaenoptera acutorostrata* (Blix and Folkow, 1995). The model estimates the SEL dose which an animal is subject to for the entire piling sequence (cumulative SEL) for different distances from the pile when the piling starts (start range), from which the animal starts to swim away. This is shown in Plate along with horizontal lines which indicate the auditory injury thresholds for different animals based on the onset of PTS for the functional hearing groups stated above from Southall et al. (2007).

47. It should be noted that this modelling was carried out for an example piling sequence to illustrate the potential for prolonged exposure to the sound. The example piling sequence does not include any gaps in the piling sequence. Previously reported piling sequences show that piling is not always continuous, often containing a number of gaps in the sequence that may last several minutes (e.g. Nedwell et al. 2007; Nedwell et al. 2009; Nedwell et al. 2010; Robinson et al. 2009a; Robinson et al. 2009b; Theobald et al. 2010; Bailey et al. 2010).

48. Furthermore, the model does not account for any time that a receptor may spend at the surface, or the reduced SEL near the surface, both of which would reduce the overall exposure. More importantly, the model cannot account for any hearing recovery which may occur, between piling strikes, during gaps in piling, or due to effective quiet, such as when the animal is near or above the surface of the water. As such, the exposure predicted in the model is likely to be an overestimate of the exposure that a receptor might be subjected to during such a piling sequence.

49. The SEL dose generally increases rapidly at close range to the pile, where the SEL received levels are substantially higher and increases less rapidly at greater ranges from the pile where the received levels are lower. Therefore, when assuming a

fleeing animal, it is the early part of the piling sequence which contributes most to the total SEL dose.

50. For receptor specific information, including marine mammal behavioural response and hearing, please refer to Chapter 12 Marine Mammal Ecology.
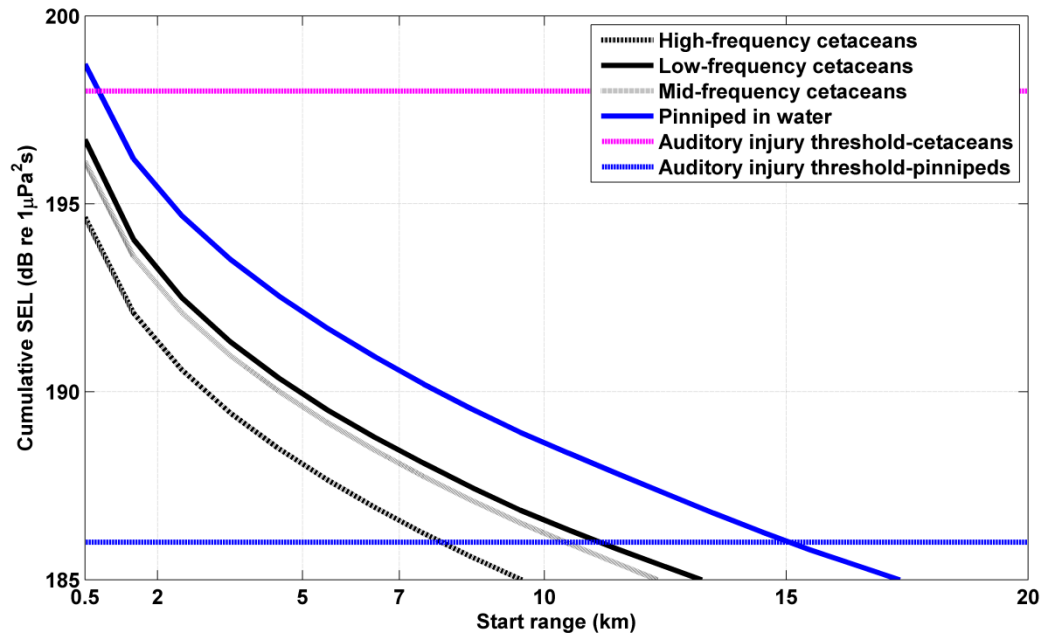

Plate 9.3. Example of an SEL dose modelling output for an illustrative piling sequence, detailed in Annex D. The cumulative SEL is indicated for various start ranges from the pile for the marine mammal functional hearing groups (Southall et al. 2007) assuming the animal starts fleeing the sound source at the onset of piling (JNCC 2010).

9.4.1.1.3   Behaviour

51. The behavioural response ranges for marine mammals, shown in Tables 9.2 to 9.5 below, were obtained using the criteria described in Chapter 12 Marine Mammal Ecology. Example noise maps for behavioural disturbance for marine mammals are also shown in Plates 9.4 to 9.8, where the contours correspond to the marine mammal behavioural disturbance criteria (described in Chapter 12 Marine Mammal Ecology). It should be noted that the longest stated impact distances only occur along limited transects from the source. Plate 9.5 shows an example of a noise footprint which may be expected for a 3,500kJ hammer energy used at the East Anglia THREE site for the harbour porpoise behavioural disturbance threshold adopted from Lucke et al. (2009).   The footprint indicates the possible spatial extent of the piling noise in terms of harbour porpoise behavioural disturbance, with no regard for specific

temporal construction sequencing across the project (see Section 9.3.3 for more detail).

52. It should be noted that the noise levels present in the water will also depend on the depth of the receptor as described in Section 9.3.5 and marine mammals near the surface will be exposed to lower noise levels with correspondingly smaller impact ranges. For example, an animal with its ears just below the water line would be exposed to substantially reduced noise levels, and even at one metre below the surface of the water, would be exposed to much lower levels than those predicted in the propagation modelling.

Table 9.2. Summary of harbour porpoise *Phocoena phocoena* (around mid-water column) impact distances estimated for pile driving during construction at the East Anglia THREE site for different hammer energies. Possible avoidance of area is stated as the minimum to the 95th percentile impact distance, where the actual impact distance within this range will depend on the transect and piling location. Larger impact distances may occur along limited transects for some locations (their approximate extent is indicated in brackets). Impact distances are rounded up to the nearest 500m for distances of 3km and less, and rounded up to the nearest 1km for distances greater than 3km.

Impact criterion	1,400kJ hammer energy	2,000kJ hammer energy	2,300kJ hammer energy	3,000kJ hammer energy	3,500kJ hammer energy
Instantaneous injury / PTS (pulse SEL 179dB re 1 $\mu Pa^2 \cdot s$)*	<500m	<500m	<500m	<1km	<1km
Fleeing response (pulse SEL 164dB re 1 $\mu Pa^2 \cdot s$)*	~3.0 to 5km	~4 to 6km	~4 to 6km	~5 to 8km	~5 to 8km
Possible avoidance of area (pulse SEL 145dB re 1 $\mu Pa^2 \cdot s$)*	~24 to 44†km (~55km)	~29 to 51†km (~58km)	~31 to 54†km (~60km)	~34 to 59†km (~66km)	~37 to 62†km (~70km)

*Lucke et al. (2009), †95th percentile impact range.

Table 9.3. Summary of mid-frequency cetacean functional hearing group (around mid-water column) impact distances estimated for pile driving during construction at the East Anglia THREE site for different hammer energies. Possible avoidance of area is stated as the minimum to the 95th percentile impact distance, where the actual impact distance within this range will depend on the transect and piling location. Larger impact distances may occur along limited transects for some locations (their approximate extent is indicated in brackets). Impact distances are rounded up to the nearest 500m for distances of 3km and less, and rounded up to the nearest 1km for distances greater than 3km.

Impact criterion	1,400kJ hammer energy	2,000kJ hammer energy	2,300kJ hammer energy	3,000kJ hammer energy	3,500kJ hammer energy
Instantaneous injury / PTS (M_{mf} weighted 198dB re 1 $\mu Pa^2 \cdot s$)*	<500m	<500m	<500m	<500m	<500m
Fleeing response (M_{mf} weighted 183dB re 1 $\mu Pa^2 \cdot s$)*	<500m	<500m	<500m	<500m	<500m
Likely avoidance of area (pulse SEL 170dB re 1 $\mu Pa^2 \cdot s$)***	~1.5 to 2.0km	~2.0 to 2.5km	~2.0 to 2.5km	~2.5 to 3.0km	~2.5 to 4km
Possible avoidance of area / Change in swimming behaviour (pulse SEL 160dB re 1 $\mu Pa^2 \cdot s$)***	~5 to 8†km (~8km)	~6 to 9†km (~10km)	~6 to 10†km (~11km)	~7 to 11†km (~12km)	~8 to 12†km (~13km)

*Southall et al. (2007) Injury Criteria, **Southall et al. (2007) Single pulse behavioural disturbance.***Southall et al. (2007) Multiple pulses severity scoring behavioural disturbance (RMS SPL converted to pulse SEL by subtraction of 10dB), †95th percentile impact range.

Table 9.4. Summary of low-frequency cetacean functional hearing group (around mid-water column) impact distances estimated for pile driving during construction at the East Anglia THREE site for different hammer energies. Possible avoidance of area is stated as the minimum to the 95th percentile impact distance, where the actual impact distance within this range will depend on the transect and piling location. Larger impact distances may occur along limited transects for some locations (their approximate extent is indicated in brackets). Impact distances are rounded up to the nearest 500m for distances of 3km and less, and rounded up to the nearest 1km for distances greater than 3km.

Impact criterion	1,400kJ hammer energy	2,000kJ hammer energy	2,300kJ hammer energy	3,000kJ hammer energy	3,500kJ hammer energy
Instantaneous injury / PTS (M_{lf} weighted 198dB re 1 $\mu Pa^2 \cdot s$)*	<500m	<500m	<500m	<500m	<500m
Fleeing response (M_{lf} weighted 183dB re 1 $\mu Pa^2 \cdot s$)*	<500m	<500m	<500m	<500m	<500m
Likely avoidance of area (pulse SEL 152dB re 1 $\mu Pa^2 \cdot s$)***	~12 to 22km	~16 to 26km	~17 to 27km	~19 to 32km	~20 to 35km
Possible avoidance of area / Change in swimming behaviour (pulse SEL 142dB re 1 $\mu Pa^2 \cdot s$)***	~34 to 57†km (~66km)	~39 to 66†km (~74km)	~40 to 69†km (~79km)	~41 to 75†km (~84km)	~42 to 79†km (~93km)

*Southall et al. (2007) Injury Criteria, **Southall et al. (2007) Single pulse behavioural disturbance.***Southall et al. (2007) Multiple pulses severity scoring behavioural disturbance (RMS SPL converted to pulse SEL by subtraction of 8dB), †95th *percentile impact range.*

Table 9.5. Summary of pinniped functional hearing group (around mid-water column) impact range estimates for pile driving during construction at the East Anglia THREE site for different hammer energies. Impact distances are rounded up to the nearest 500m for distances of 3km and less, and rounded up to the nearest 1km for distances greater than 3km.

Impact criterion	1,400kJ hammer energy	2,000kJ hammer energy	2,300kJ hammer energy	3,000kJ hammer energy	3,500kJ hammer energy
Instantaneous injury / PTS * (M_{pw} weighted 186dB re 1 $\mu Pa^2 \cdot s$)	<500m	<500m	<500m	<500m	<500m
Fleeing response / Likely avoidance (M_{pw} weighted 171dB re 1 $\mu Pa^2 \cdot s$) **	<1.5km	<1.5km	<2.0km	<2.0km	<2.5km

*Southall et al. (2007) Injury Criteria, **Southall et al. (2007) Single pulse behavioural disturbance.

Plate 9.4. Single pile propagation model output (see Section 9.3.2 for details) for a 3,500 kJ hammer strike energy at the East Anglia THREE site (example location based on Location ID17, Table 9.9, Annex C), where the 145 and 164 dB re 1µPa²s SEL contours correspond to possible avoidance of area and fleeing, respectively, for harbour porpoise. White indicates a depth of < 0 m for tidal height modelled (HAT).

Plate 9.5. An example of a noise footprint model output (see Section 9.3.3 for details) for a 3,500 kJ hammer strike energy at the East Anglia THREE site, where the contours correspond to the behavioural disturbance criteria for harbour porpoise behavioural disturbance (described in Chapter 12 Marine Mammal Ecology). White indicates a depth of < 0 m for tidal height modelled (HAT).
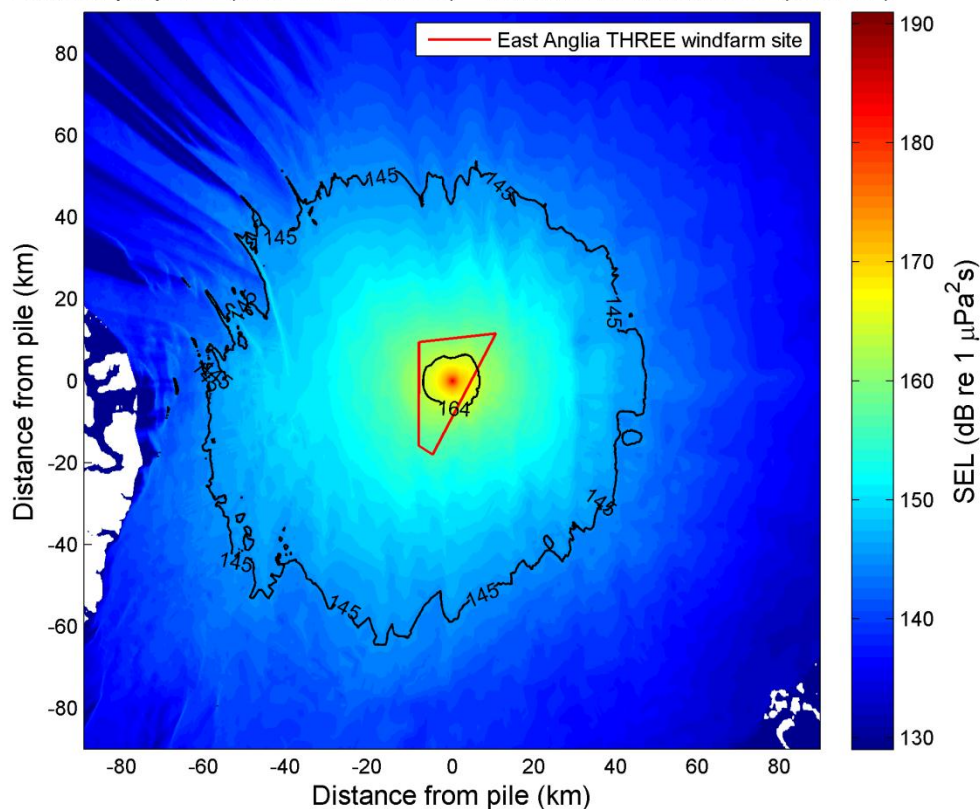
Plate 9.6. Single pile propagation model output (see Section 9.3.2 for details) for a 3,500 kJ hammer strike energy at the East Anglia THREE site (example location based on Location ID17, Table 9.9, Annex C), where the 160 and 170 dB re 1µPa²s SEL contours correspond to possible avoidance of area/change in swimming behaviour and likely avoidance of area, respectively, for mid-frequency cetaceans. White indicates a depth of < 0 m for tidal height modelled (HAT).
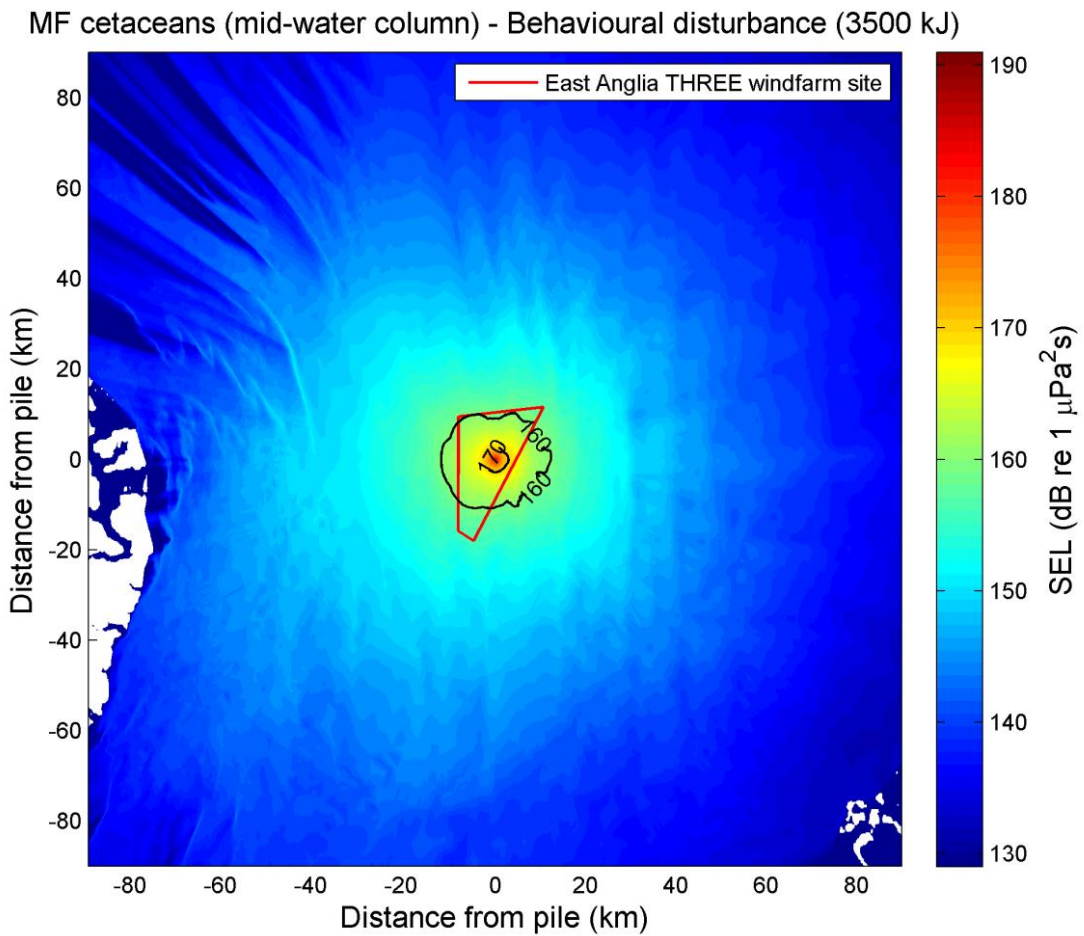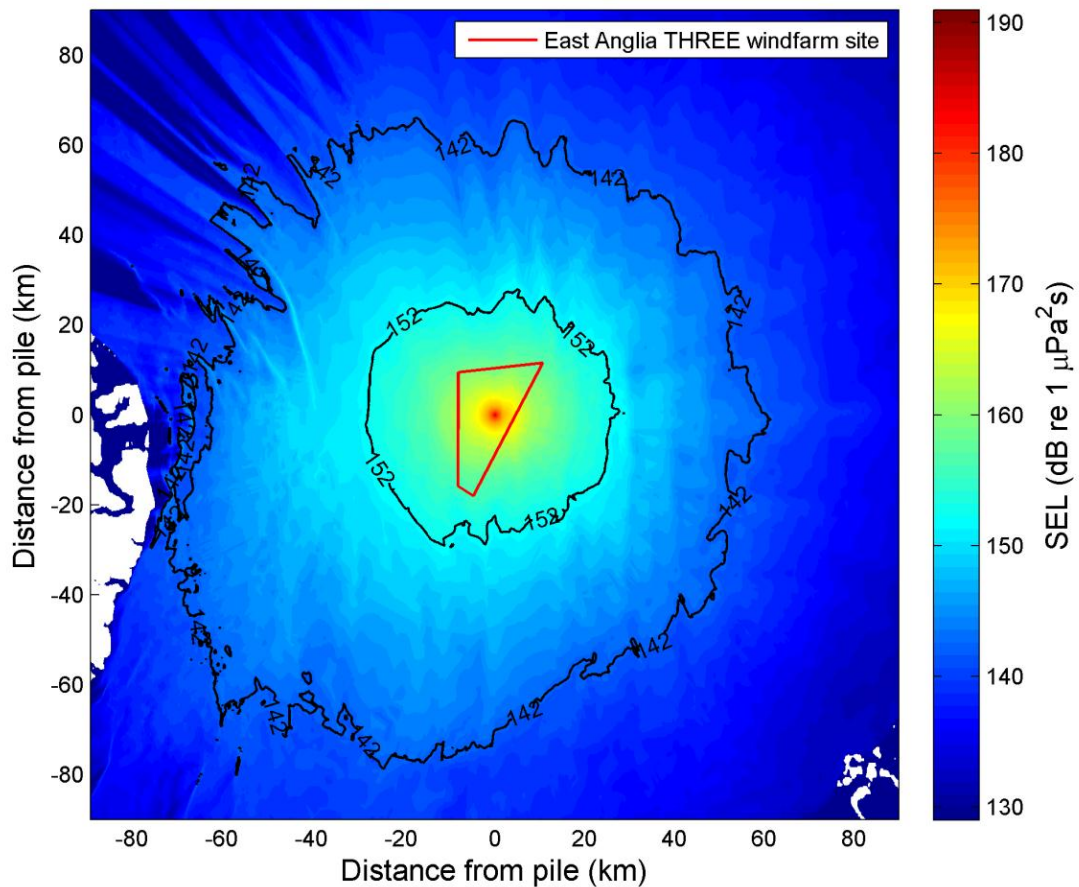
Plate 9.7. Single pile propagation model output (see Section 9.3.2 for details) for a 3,500 kJ hammer strike energy at the East Anglia THREE site (example location based on Location ID17, Table 9.9, Annex C), where the 142 and 152 dB re 1µPa²s SEL contours correspond to possible avoidance of area/change in swimming behaviour and likely avoidance of area, respectively, for low-frequency cetaceans. White indicates a depth of < 0 m for tidal height modelled (HAT).
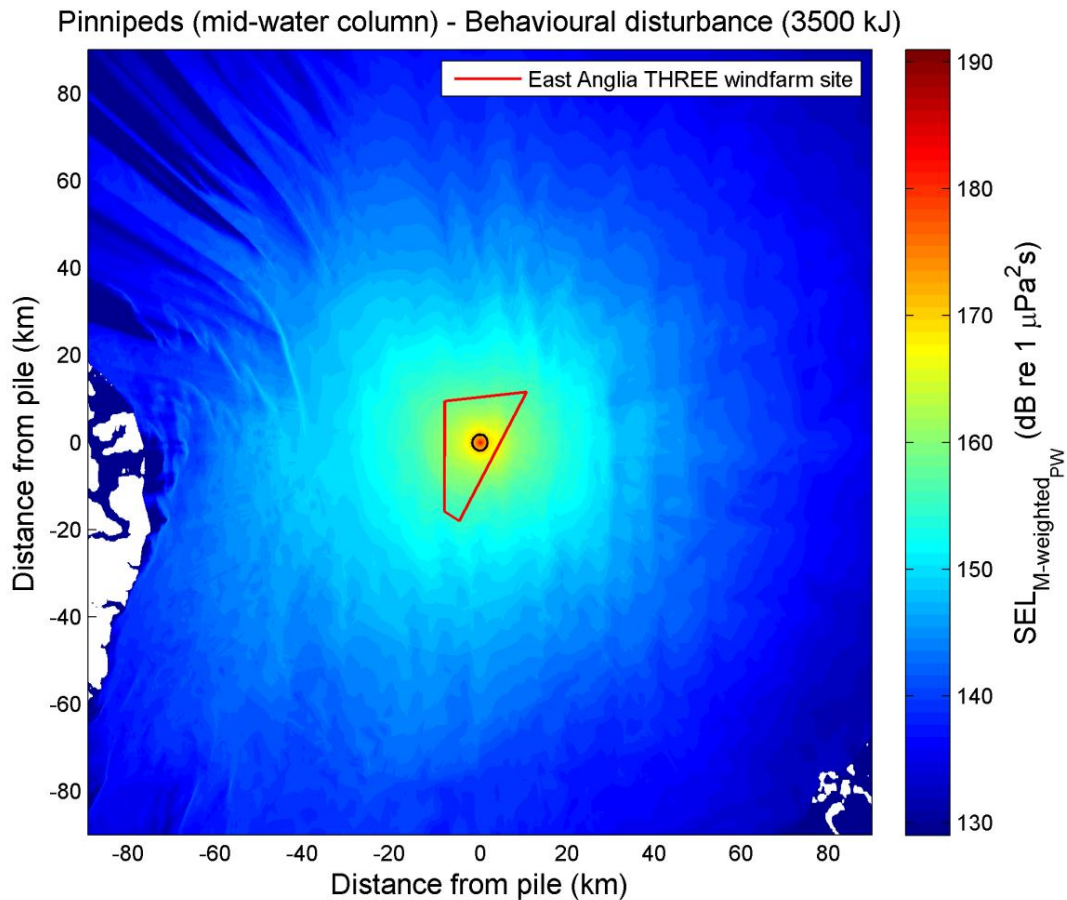
Plate 9.8. Single pile propagation model output (see Section 9.3.2 for details) for a pinniped indicating possible fleeing response (based on instantaneous TTS) for a 3,500 kJ hammer strike energy at the East Anglia THREE site (example location based on Location ID17, Table 9.9, Annex C). White indicates a depth of < 0 m for tidal height modelled (HAT).

9.4.1.2 Fish

9.4.1.2.1 Injury

53. The fish injury criteria adopted for this assessment are outlined in detail in Chapter 11 Fish and Shellfish Ecology and the estimated potential instantaneous injury ranges for fish based on this criteria are shown in Tables 9.6 and 9.7. Mortality is not shown but may be expected to only be likely to occur in extreme proximity to the pile. Prolonged exposure to repeated hammer strikes (SEL dose) may increase the distance over which there would be a risk of injury. If it is assumed that the fish move away from the pile during installation then the risk of injury due to prolonged exposure, and therefore the injury range, would be reduced. For fish larvae, the risk of mortality due to prolonged noise exposure could be reduced by any drift of larvae due to water currents and may reduce the risk of mortality. It is however, not possible to establish if mortality might occur or indeed at what range from the pile, as the work by Bolle et

al. (2011 and 2012) was unable to induce a statistically significant change in survival rates of fish larvae following a prolonged exposure with a substantial SEL dose.

9.4.1.2.2 Behaviour

54.   The ranges over which behavioural disturbance is estimated to occur are based on criteria outlined in detail in Chapter 11 Fish and Shellfish Ecology. These are presented for fish around mid-water column in Table 9.6 and for fish near the sea bed in Table 9.7. The levels for fish near the sea bed were calculated using a broadband correction, established using the modelling to establish the sound pressure as a function of position in the water column and described in Section 9.3.5, to the levels predicted using the energy flux model described in Section 9.3.2. Example noise maps for behavioural disturbance for fish are also shown in Plates 9.9 and 9.10.

55.   As can be seen in Plates 9.9 and 9.10 there is variation in the distances where general behavioural response for fish may be expected around the East Anglia THREE site, depending on the bearing from the source, which reflects the changes in bathymetry. Favourable sound propagation conditions to the west of the East Anglia THREE site mean that the impact ranges are generally larger towards the south-west to north-west of the East Anglia THREE site. In general, the deeper water areas also result in larger impact ranges for behavioural disturbance. Plates 9.11 and 9.12 show the potential noise footprint which is predicted for fish. This shows the possible spatial extent of the piling noise in terms of fish behavioural disturbance, with no regard for specific temporal construction sequencing across the project (see Section 9.3.3 for more detail).

56.   It should be noted that no long-term observational studies have been reported in the literature to assess the response of fish populations to marine impact piling and so any fish behaviour impact criteria should strictly only be used for guidance.

Table 9.6. Summary of impact distances for fish around mid-water column (e.g. pelagic fish), estimated for pile driving during construction at the East Anglia THREE site for different hammer energies. Behavioural disturbance of area is stated as the minimum to the 95th percentile impact distance, where the actual impact distance within this range will depend on the transect and piling location. Larger impact distances may occur along limited transects for some locations (their approximate extent is indicated in brackets). Impact distances are rounded up to the nearest 50m for distances of 500m and less, up to the nearest 500m for distances of 3km and less, and up to the nearest 1km for distances greater than 3km.

Impact criterion	1,400kJ hammer energy	2,000kJ hammer energy	2,300kJ hammer energy	3,000kJ hammer energy	3,500kJ hammer energy
Instantaneous injury (peak pressure level 206dB re 1 μPa)	<100m	<150m	<150m	<200m	<250m
Startle response (peak pressure level 200dB re 1 μPa)	<350m	<500m	<500m	<1.0km	<1.0km
Behavioural disturbance (peak pressure level 168 - 173dB re 1 μPa)	~10 to 25†km (~28km)	~12 to 30†km (~35km)	~12 to 32†km (~37km)	~14 to 37†km (~44km)	~16 to 40†km (~48km)

†95th percentile impact range.

Table 9.7. Summary of impact distances for fish near the sea bed (e.g. demersal fish), estimated for pile driving during construction at the East Anglia THREE site for different hammer energies. Behavioural disturbance of area is stated as the minimum to the 95th percentile impact distance, where the actual impact distance within this range will depend on the transect and piling location. Larger impact distances may occur along limited transects for some locations (their approximate extent is indicated in brackets). Impact distances are rounded up to the nearest 50m for distances of 500m and less, up to the nearest 500m for distances of 3km and less, and up to the nearest 1km for distances greater than 3km.

| Impact criterion	1,400kJ hammer energy	2,000kJ hammer energy	2,300kJ hammer energy	3,000kJ hammer energy	3,500kJ hammer energy
Instantaneous injury (peak pressure level 206dB re 1 μPa)	<100m	<150m	<150m	<200m	<250m
Startle response (peak pressure level 200dB re 1 μPa)	<350m	<500m	<500m	<1.0km	<1.0km
Behavioural disturbance (peak pressure level 168 - 173dB re 1 μPa)	~7 to 20†km (~22km)	~9 to 23†km (~26km)	~10 to 24†km (~27km)	~10 to 27†km (~31km)	~11 to 30†km (~34km)

†95th percentile impact range.
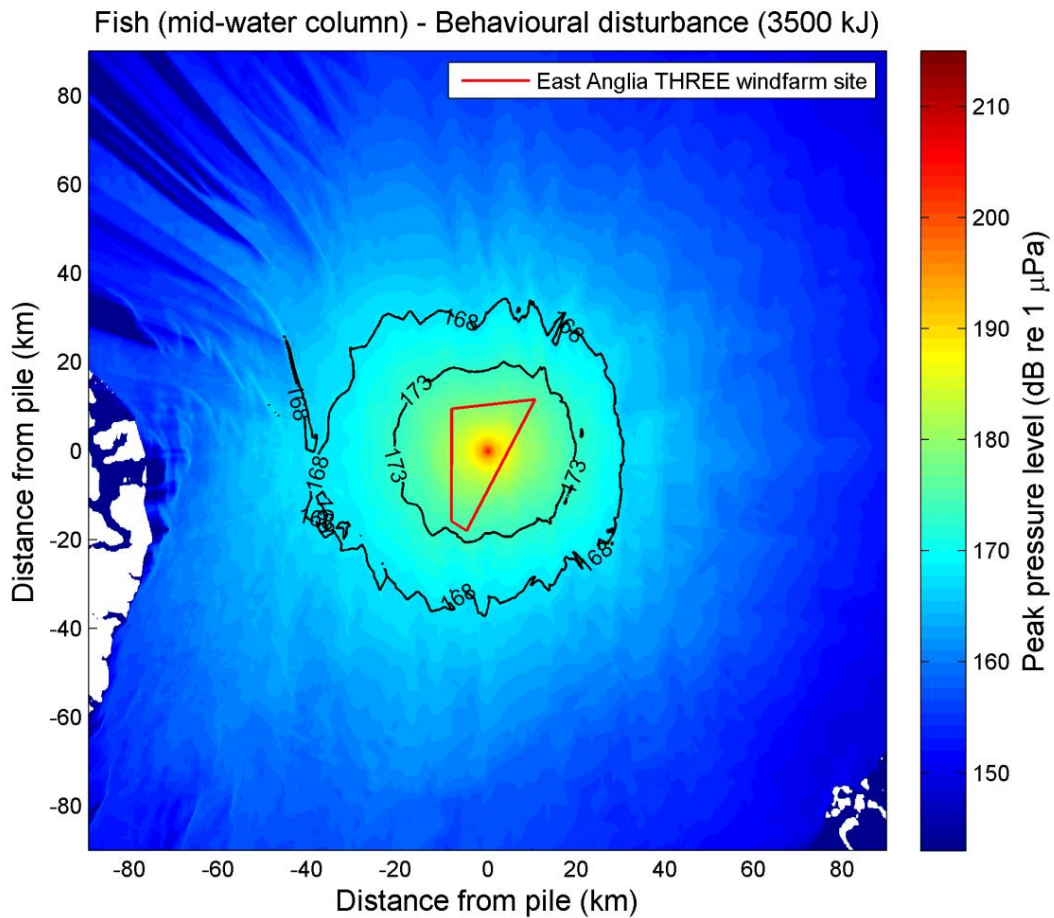
Plate 9.9. Single pile propagation model output (see Section 9.3.2 for details) for pelagic fish (fish near mid-water column) behavioural disturbance contours for a 3,500 kJ hammer strike energy at the East Anglia THREE site (example location based on Location ID17, Table 9.9, Annex C). White indicates a depth of < 0 m for tidal height modelled (HAT).

Plate 9.10. Single pile propagation model output (see Section 9.3.2 for details) for demersal fish (fish near sea bed) behavioural disturbance contours for a 3,500 kJ hammer strike energy at the East Anglia THREE site (example location based on Location ID17, Table 9.9, Annex C). White indicates a depth of < 0 m for tidal height modelled (HAT).

Plate 9.11. Noise footprint model output (see Section 9.3.3 for details) for pelagic fish (fish near mid-water column) behavioural disturbance contours for a 3,500 kJ hammer strike energy at the East Anglia THREE site. White indicates a depth of < 0 m for tidal height modelled (HAT).
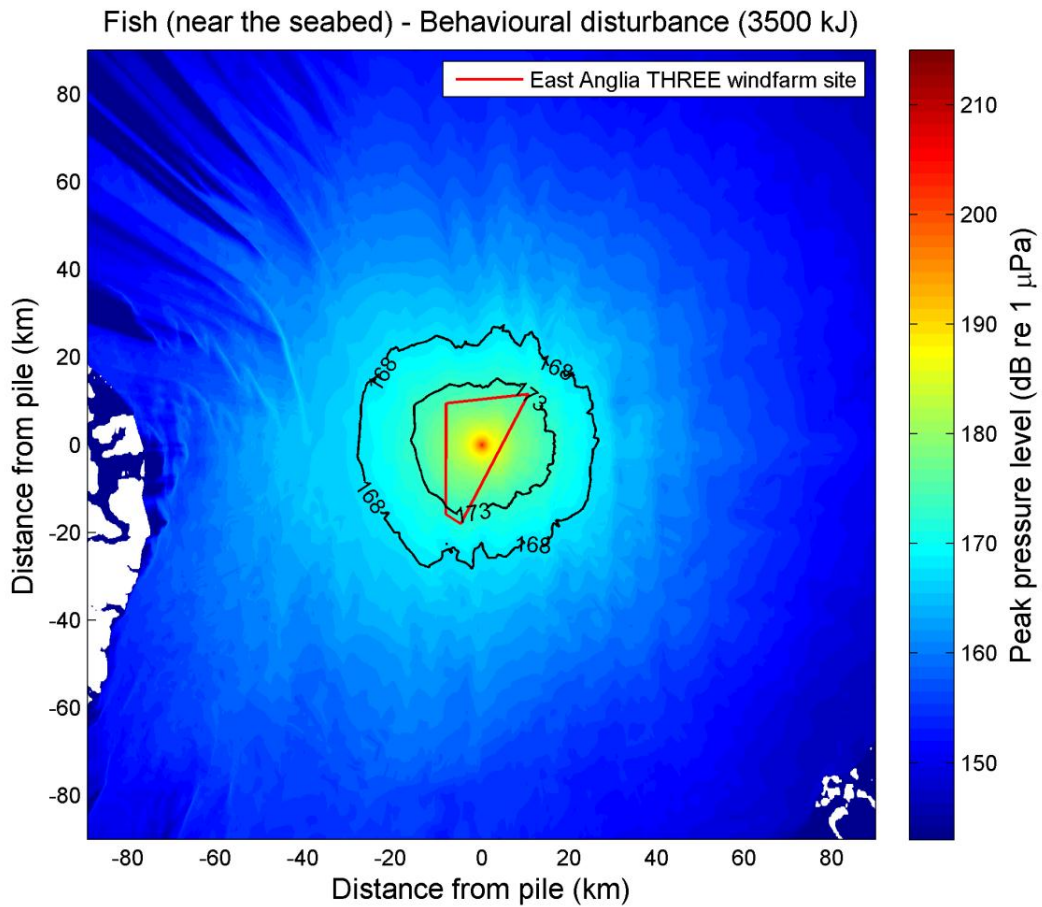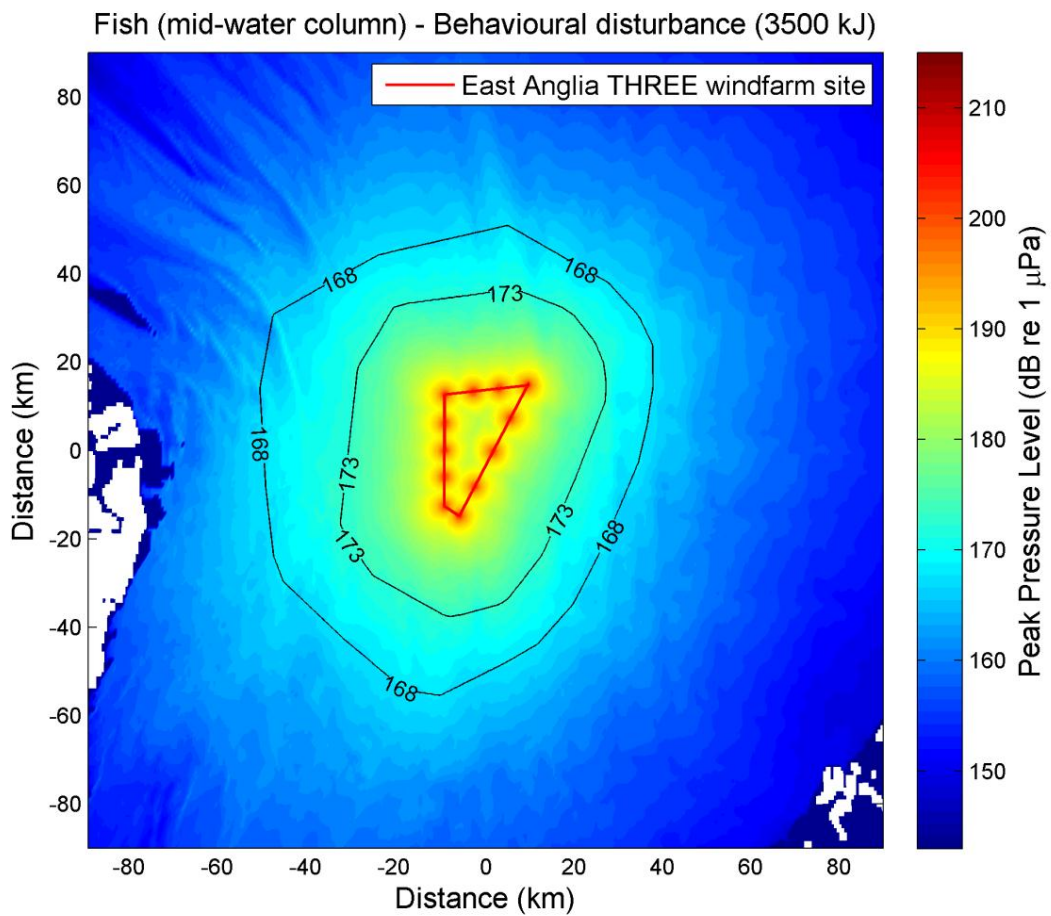
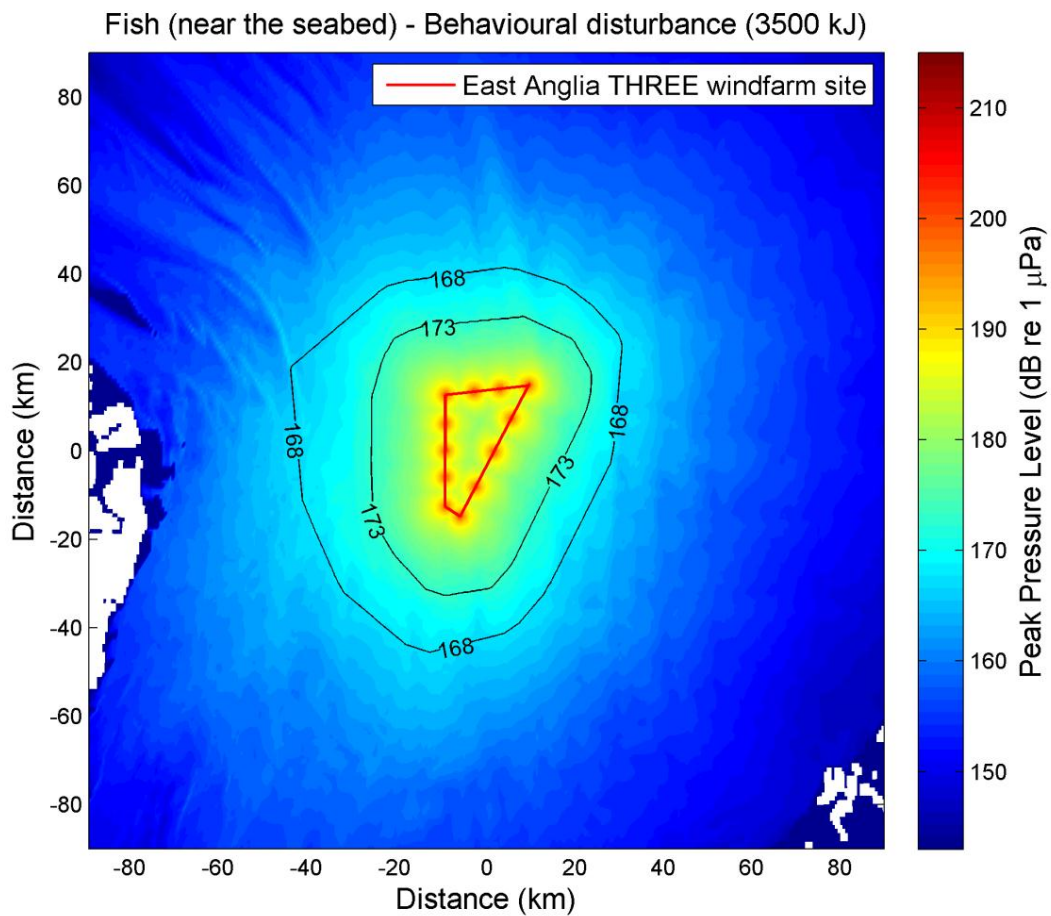Fish (near the seabed) - Behavioural disturbance (3500 kJ)

Plate 9.12. Noise footprint model output (see Section 9.3.3 for details) for demersal fish (fish near sea bed) behavioural disturbance contours for a 3,500 kJ hammer strike energy at the East Anglia THREE site. White indicates a depth of < 0 m for tidal height modelled (HAT).

9.4.1.3   Effect of using Multiple Piling Vessels

57.   The effect on the noise levels generated from the use of multiple piling vessels within the East Anglia THREE site has been modelled using the methodology described in Section 9.3.4. This modelling considered the use of two piling vessels operating concurrently in the East Anglia THREE site, both, in relative proximity to each other (~4km separation), and at opposite ends of the site (~33km separation).

58.   Plates 9.13 and 9.14 show examples of the modelled scenario for a hammer blow energy of 3,500kJ. Contour lines are shown to help illustrate the potential difference in impacted area when using multiple piling vessels with different separations. The contours in Plates 9.13 and 9.14 correspond to the harbour porpoise behavioural disturbance criteria (described in Chapter 12 Marine Mammal Ecology) and fish behavioural disturbance (described in Chapter 11 Fish and Shellfish Ecology),

respectively. As it is highly unlikely that the sound pulses would interfere constructively, the sound levels would not be expected to increase as a result of summation, thus the impact ranges stated in Table 9.2 to 9.5, for marine mammals, and Tables 9.6 and 9.7 for fish, are still relevant to each individual pile location.

59. Although the use of multiple piling vessels may increase the impacted area at any given time, it also reduces the overall construction time without necessarily increasing the total impacted area over the construction period of the windfarm. However, the increased extent of the impacted area, particularly if the piling vessels are a substantial distance apart, may result in an increased short-term impact at the time of construction, which may have consequences in terms of receptor displacement. It may also increase the total SEL dose. It should be noted that the worst-case scenario may depend on the receptor (see Chapter 11 Fish and Shellfish Ecology and Chapter 12 Marine Mammal Ecology for fish and marine mammals, respectively).

Plate 9.13. Underwater noise modelling for two concurrently operating piling vessels within the East Anglia THREE site each operating with a 3,500kJ hammer blow energy. The left panel illustrates two piling vessels operating in the same part of the windfarm (approximately 4 km apart) and the right panel illustrates two piling vessels operating at geographical extremities of the windfarm (approximately 33 km apart). Contour lines indicate possible behavioural disturbance based on criteria for harbour porpoise (described in Chapter 12 Marine Mammal Ecology). White indicates a depth of < 0 m for tidal height modelled (HAT).
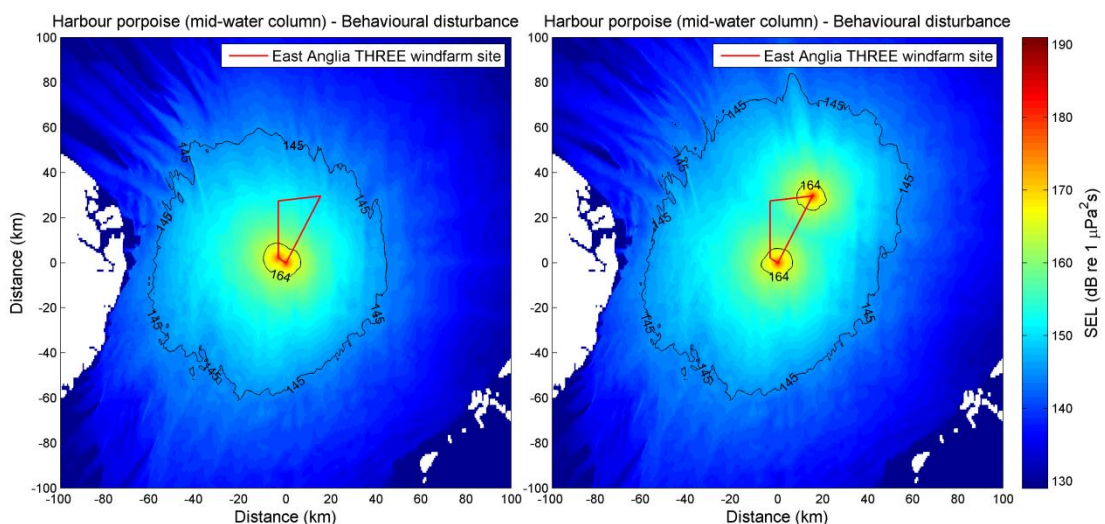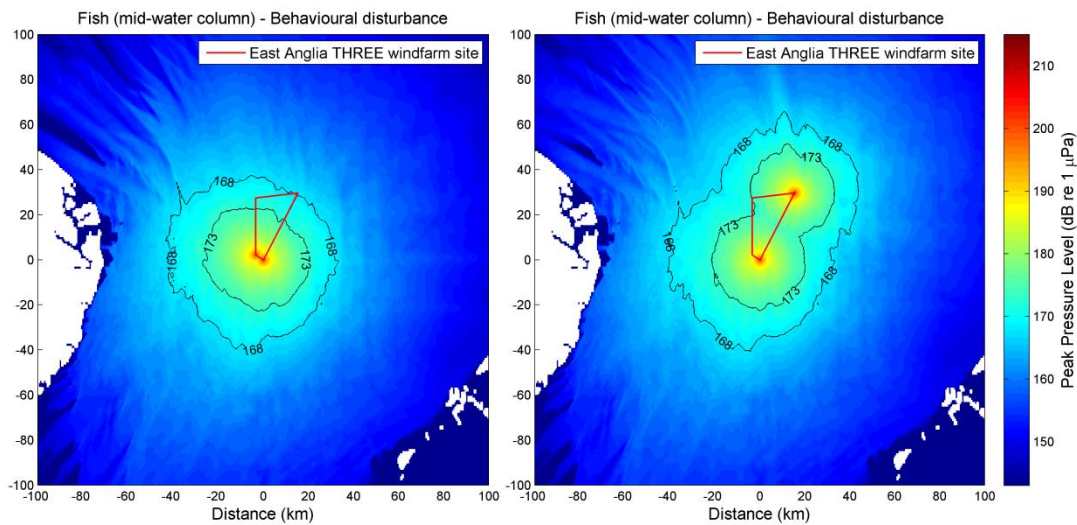
Plate 9.14. Underwater noise modelling for two concurrently operating piling vessels within the East Anglia THREE site each operating with a 3,500kJ hammer blow energy. The left panel illustrates two piling vessels operating in the same part of the windfarm (approximately 4 km apart) and the right panel illustrates two piling vessels operating at geographical extremities of the windfarm (approximately 33 km apart). Contour lines indicate possible behavioural disturbance, around mid-water column, based on criteria for fish (described in Chapter 11 Fish and Shellfish Ecology). White indicates a depth of < 0 m for tidal height modelled (HAT).

9.4.2 Operational Phase

60. There are very few reported measurements of wind turbine noise and much of the data that is publicly available is summarised in Wahlberg and Westerberg (2005) and Madsen et al. (2006), with Tougaard and Henriksen (2009) providing a more recent update.

61. Underwater noise from an operational wind turbine mainly originates from the gearbox and the generator, and has tonal characteristics (Madsen et al. 2006; Tougaard and Henriksen 2009). The radiated levels are relatively low and the spatial extent of the potential impact of the operational windfarm noise on marine receptors is generally estimated to be small, and wind turbine noise has generally been considered unlikely to result in any injury to marine mammals (e.g. Tougaard and Henriksen 2009) or fish (Wahlberg and Westerberg 2005).

62. Previous studies have reported behavioural response to only be likely to occur at close ranges from the wind turbine (a few metres for fish and harbour porpoise (Wahlberg and Westerberg 2005 and Tougaard and Henriksen 2009, respectively) and possibly up to a few hundred metres for seals (Tougaard and Henriksen 2009). Touggard and Henriksen (2009) further show that even masking from operational noise is unlikely to impact harbour porpoise and seal acoustic communication due to the low frequencies and low levels produced.

63.   The information available in the scientific literature regarding the effect of operational wind turbines is extremely limited, and this is also true for other sources of continuous noise. The International Council for the Exploration of the Sea (ICES) has formulated recommendations for maximum radiated underwater noise from research vessels which are approximately 30dB above the hearing threshold of Atlantic cod and herring (ICES:209 1995). The implication of this is that the presence of continuous noise that is not significantly above the hearing threshold of fish is not thought to cause any significant movement of fish away from the source. In studies of very low frequency sound, Sand et al. (2001) indicate that consistent deterrence from the source is only likely to occur at particle accelerations equivalent to a free-field SPL of 160dB re 1 μPa (RMS). This is higher than the noise levels reported in the open literature for operational windfarms measured at a number of ranges, all within a few hundred metres of the wind turbine (Nedwell et al. 2007; Edwards et al. 2007; Betke et al. 2004, see also Wahlberg and Westerberg 2005 and Madsen et al. 2006). The particle acceleration resulting from an operational wind turbine has also been measured by Sigray et al. (2011) with the resultant levels being considered too low to be of concern for behavioural reactions from fish. Furthermore, the particle acceleration levels measured at 10m from the wind turbine were comparable with hearing thresholds. However, the available measurement data is mostly for smaller wind turbines (up to 1.5MW) and it may be expected that larger wind turbines could result in different acoustic characteristics, with foundation type also having an influence on the acoustic characteristics of the noise radiated from the structure (e.g. Marmo et al. 2013).

64.   Noise would also result from surface vessels servicing the windfarm. However, noise levels reported by Malme et al. (1989) and Richardson et al. (1995) for large surface vessels indicate that physiological damage to marine fauna is unlikely, although the levels could be sufficient to cause local disturbance of sensitive marine fauna in the vicinity of the vessel, depending on ambient noise levels.

65.   Considering previously reported data on the operational wind turbine noise of a windfarm and the likely noise from any associated service vessels, any increase in the ambient noise levels in the area surrounding the windfarm site might be expected to be relatively small and would be dependent on noise associated with near-by shipping lanes and other sources of ambient noise. It should also be noted that a major contribution to the ambient noise would result from sea-state, which would be expected to increase as the wind turbine rotational speed increases with wind speed. Increased ambient noise may exceed the wind turbine noise, as has been observed by Tougaard and Henriksen (2009). Modelling of the noise radiated by operational wind turbines by Marmo et al. (2013) shows potential for variation between foundation

types but reports underwater noise levels which are broadly consistent with previously measured data.

9.4.3   Decommissioning

66.   Temporarily elevated underwater noise levels might be expected during the decommissioning phase due to increased vessel movements and removal of the wind turbine foundations. The resulting noise levels will depend on the method used for removal of the foundation. For abrasive cutting, often anticipated for wind turbine removal, the noise level would not be expected to be significantly higher than general surface vessel noise. Studies of underwater construction noise (decommissioning) report source level which are similar to those reported for medium sized surface vessels and ferries (Malme et al. 1989; Richardson et al. 1995).

9.5   Summary

67.   This report describes the underwater noise modelling undertaken to assess the likely underwater noise levels generated by the installation of wind turbine foundations at the East Anglia THREE site in support of the Environmental Impact Assessment. Marine impact piling is considered to be the most prevalent source of high amplitude underwater noise during the development of an offshore windfarm, with potential for an impact on marine fauna.

68.   Multiple foundation locations were modelled representing a range of water depths and bathymetry profiles across the site. The modelled sources were based on the use of various hammer blow energies that may be used during construction at the East Anglia THREE site, ranging from 1,400kJ to 3,500kJ, with 3,500kJ being the maximum hammer energy modelled. The propagation model used was based on an energy flux approach and provided SEL and peak pressure received level output as a function of range away from each modelled location whilst accounting for sea bed properties and varying bathymetry.

69.   The outputs of the underwater noise modelling has been used to predict the potential impact ranges for marine mammals and fish during pile driving, based on injury and behaviour criteria specified in Chapter 12 Marine Mammal Ecology and Chapter 11 Fish and Shellfish Ecology, respectively.

70.   There is considerable variability in the extent of impact ranges across the East Anglia THREE site due to variable bathymetry, with the greatest ranges observed to the west (south-west to north-west) of the site.

71.   The effect of multiple piling vessels for simultaneous pile driving has also been modelled to illustrate the effect of vessel separation distance on the potential

impacted area. As the instantaneous sound pressure is highly unlikely to add up in such a way as to increase the peak noise level, the size of the impacted area is dependent on the separation between the vessels.

72. Possible noise from the operation of the windfarm has also been discussed based on previously published measurement data and suggests that broadband noise levels within the boundary of a windfarm are not likely to be significantly above ambient noise, although the operation of the wind turbines may increase the ambient noise slightly during periods of light winds, calm seas and low shipping traffic, assuming that the wind is sufficient to turn the wind turbines.

9.6 References

Akamatsu, T., Teilmann, J., Miller, L.A., Tougaard, J., Dietz, R., Wand, D., Wand, K., Siebert, U. and Naito Y. (2007) Comparison of echolocation behaviour between coastal and riverine porpoises. *Deep-sea Res*. 54: 290-297.

Ainslie, M. A., Harrison, C. H. and Burns, P. W. (1994) Reverberation modelling with INSIGHT. *Proc Institute of Acoustics*, 16, (6), 105-112.

Ainslie, M. A., de Jong, C. A. F., Dol., H. S., Blacquière, G. and Marasini, C. (2009) *Assessment of natural and anthropogenic sound sources and acoustic propagation in the North Sea*. TNO Report TNO-DV 2009 C084.

Ainslie, M. A. (2011) *Standard for measuring and monitoring of underwater noise, Part 1: Physical quantities and their units*. TNO Report, TNO-DV 2011 C235, September 2011.

Ainslie, M. A., de Jong, C. A. F., Robinson, S. P., Lepper, P. A. (2012) What is the source level of pile driving noise in water?. *The Effects of Noise on Aquatic Life: Advances in Experimental Medicine and Biology*, 730, pp.445-448, DOI: 10.1007/978-1-4419-7311-5_100.

Bailey, H., Senior, B., Simmons, D., Rusin, J., Picken, G. and Thompson, P. M. (2010) Assessing underwater noise levels during pile-driving at an offshore wind farm and its potential effects on marine mammals, *Marine Pollution Bulletin*, 60, pp. 888-897.

Betke, K., Glahn, M. S-v. and Matuschek, R. (2004) Underwater noise emissions from offshore wind turbines. *Proceedings of CFA/DAGA '04*.

Blix, A. S., and Folkow, L. (1995) Daily energy requirements in free living minke whales. *Acta Physiol. Scand.* 153, 61-66.

Bolle, L. J., de Jong, C. A. F., Bierman, S., de Hann, D., Huijer, T., Kaptein, D., Lohman, M., Tribuhl, S., van Beek, P., van Damme, C. J. G., van den Berg, F., van der Heul, J., van Keeken,

O., Wessels, P. and Winter, E. (2011) *Effect of piling noise on the survival of fish larvae (pilot study)*. IMARES Report number CO92/11.

Bolle, L. J., de Jong, C. A. F., Bierman, S., van Beek, P., van Keeken, O., Wessels, P., van Damme, C. J. G., Winter, E., de Hann, D. and Dekeling, R. P. A. (2012) Common Sole Larvae Survive High Levels of Pile-Driving Sound in Controlled Exposure Experiments. *PLoS ONE*, 7(3), pp.e33052 doi:10.1371/journal.pone.0033052.

Carey, W. M. (2006) Sound sources and levels in the ocean. *IEEE Journal of Oceanic Engineering*, 31 (1), pp 61-74.

Coates, R. (1988) An Empirical Formula for Computing the Beckmann-Spizzichino Surface Reflection Loss Coefficient. *IEEE Trans Ultrason. Ferroelectr. Freq. Control*, 35(4), 522-523.

Collins, M. D. (1993) A split-step Pade solution for parabolic equation method. *J. Acoust. Soc. Am.*, 93, pp. 1736-1742.

Culik, B.M., Koschinski, S., Tregenza, N. and Ellis G.M. (2001) Reactions of harbour porpoise *Phocoena phocoena* and herring *Clupea harengus* to acoustic alarms, *Mar.Ecol,.Prog. Ser*., 2011: 255-260.

de Jong C. A. F. and Ainslie M. A. (2008) Underwater radiated noise due to the piling for the Q7 offshore wind park. *Proceedings of Acoustics 08*, Paris.

DECC (2014) [Online] Available at: https://www.gov.uk/oil-and-gas-offshore-maps-and-gis-shapefiles [Accessed 25 March 2014].

Degraer, S., Brabant, R. and Rumes, B. (2010) *Offshore wind farms in the Belgium part of the North Sea, Chapter 4, Underwater noise produced by the piling activities during the construction of the Belwind offshore wind farm (Bligh Bank, Belgian marine water),* by A. Norro, J. Haelters, B. Rumes and S. Degraer, 2010.

Edwards, B., Brooker, A., Workman, R., Parvin, S. J. and Nedwell, J. R. (2007) *Subsea operational noise assessment at the Barrow Offshore Wind Farm site*. Subacoustech Report No. 753R0109.

Ferla, C. M., Porter, M. B., Jensen F. B. (1996). *C-SNAP: Coupled SACLANTCEN normal mode propagation loss model*. SACLANTCEN Memorandum SM-274, Dec. 1993. SACLANT Undersea Research Centre, La Spezia.

Goh, J. T. and Schmidt, H. (1996). A hybrid coupled wave-number integration approach to range-dependent seismo-acoustic modelling. *J. Acoust. Soc. Am.*, 100:1409-1420, 1995.

Hamilton, E. L. (1980) Geoacoustic modelling of the sea floor. *J. Acoust. Soc. Am.*, vol. 68(5), pp. 1313-1340.

Hawkins, A. (2009) The impact of pile driving upon fish. *Proc. Inst. Acoustics*, vol.31. pt.1, pp. 72-79.

Hazelwood, R. A. (2012) Ground Roll Waves as a Potential Influence on Fish: Measurement and Analysis Techniques, Advances in Experimental Medicine and Biology, 730, pp. 449-452. DOI: 10.1007/978-1-4419-7311-5_101.

ICES:209 (1995) ICES Cooperative Research Report No. 209 '*Underwater Noise of Research Vessels*'

Jensen, F. B., Kuperman, W. A., Porter, M. B. and Schmidt, H. (2000) *Computational Ocean Acoustics*, AIP press Springer-Verlag, ISBN: 1-56396-209-8, p 36-37.

JNCC (2010) *Statutory nature conservation agency protocol for minimizing the risk of injury to marine mammals from piling noise*. JNCC, August 2010.

Kaye, G. W. C. and Laby, T. H. (2004) *Tables of Physical and Chemical Constants*. (Available online at: http://www.kayelaby.npl.co.uk/).

Kinsler, L. E., Frey, A. R., Coppens, A. B and Sanders. J. V. (1982) *Fundamentals of Acoustics*, (3rd edition), Wiley.

Lepper, P. A., Pangerc, T. Robinson, S. P. and Theobald, P. D. (2011) Theoretical comparison of cumulative sound exposure estimates from jacket and tripod foundation construction. *Proceedings 4th International Conference on Underwater Acoustic Measurement: Technologies and Results*. pp. 731-737.

Lucke, K., Siebert, U., Lepper, P. A. and Blanchet, M. A. (2009) Temporary shift in masked hearing thresholds in a harbor porpoise (*Phocoena phocoena*) after exposure to seismic airgun stimuli, *J. Acoust. Soc. Am.*, 125 (6), pp. 4060-4070.

Lurton, X. *An introduction to underwater acoustics*, Elsevier, 2003.

Madsen, P. T. (2005) Marine mammals and noise: problems with root mean square sound pressure for transients", *J. Acoust. Soc. Am.*, 117, pp. 3952-3956.

Madsen, P. T., Wahlberg, M., Tougaard, J, Lucke, K. and Tyack P. (2006) Wind turbine underwater noise and marine mammals: implications of current knowledge and data needs. *Mar. Ecol. Prog. Ser.*, 309, pp. 279 – 294.

Maggi, A. L. and Duncan, A. J. (2010) *Underwater Acoustic Propagation Modelling software – AcTUP V2.2L. Centre for Marine Science and Technology (CMST), Curtin University of Technology in Australia, (2010).

Malme, C. I., Miles, P. R., Miller, G. W., Richardson, W. J., Reseneau, D. G., Thomson, D. H., Greene, C. R. (1989) *Analysis and ranking of the acoustic disturbance potential of petroleum industry activities and other sources of noise in the environment of marine mammals in Alaska*, BBN Report No. 6945 OCS Study MMS 89-0005. Reb. From BBN Labs Inc., Cambridge, MA, for U.S. Minerals Managements Service, Anchorage, AK. NTIS PB90-188673.

Marmo B., Roberts I., Buckingham M.P., King S., and Booth C. (2013) Modelling of noise effects of operational offshore wind turbines including noise transmission through various foundation types. Edinburgh: Scottish Government.

Medwin, H. and Clay, C. (1998) *Fundamentals of Acoustical Oceanography*. Academic Press, Boston.

MSFD (2008) *Marine Strategy Framework Directive*. Directive 2008/56/EC of the European Parliament and of the Council. 17 June 2008, Commission Decision of 1st September 2010, Official Journal of the European Union, L232/14.

NPS EN-1 (2011) *Overarching National Policy Statement for Energy (EN-1)*, DECC, July 2011.

NPS EN-3 (2011) National Policy Statement for Renewable Energy Infrastructure (EN-3), DECC, July 2011.

Nedwell, J. R., Turnpenny, A. W. H., Lovell, J. M. and Edwards, B. (2006) An investigation into the effects of underwater piling noise on salmonids. *J. Acoust. Soc. Am.*, 120, pp. 2550-2554.

Nedwell, J. R., Parvin, S. J., Edwards, B., Workman, R., Brooker, A. G. and Kynoch, J. E. (2007) *Measurement and Interpretation of Underwater Noise During Construction and Operation of Wind Farms in UK Waters*. Subacoustech Report No. 544R0738 to COWRIE Ltd. ISBN: 978-0-9554279-5-4.

Nedwell, J. R., Brooker, A. G., Cummins, D, and Barham, R. (2009) *Thanet Offshore Wind Farm Measurement and assessment of underwater noise during impact piling operations to install monopile foundations*. Royal Haskoning, Final report 9T6750, September 2009.

Nedwell, J. R., Brooker, A. G., Cummins, D, and Barham, R. (2010) *Thanet Offshore Wind Farm Measurement and assessment of underwater noise during impact piling operations to install monopile foundations*. Royal Haskoning, Final report Version 2 9T6750, July 2010.

Nehls, G., Betke, K., Eckelmann, S. and Ros, M. (2007) *Assessment and costs of potential engineering solutions for the mitigation of the impacts of underwater noise arising from the construction of offshore windfarms*. BioConsultSH report, Husum, Germany. On behalf of COWRIE Ltd.

NOAA (2013), *Draft Guidance for Assessing the Effects of Anthropogenic Sound on Marine Mammals, Acoustic threshold levels for Onset of Permanent and Temporary Threshold Shifts*. 2013, pp. 76, For updates see: http://www.nmfs.noaa.gov/pr/acoustics/guidelines.htm

Otani, S., Naito, Y., Kato, A. and Kawamura, A. (2000) Diving behaviour and swimming speed for free-ranging harbour porpoise, *Phocean phocena*. *Marine Mammal Science*, l6(4), pp. 811-814.

Richardson, W. J., Greene, C. R. J., Malme, C. I. and Thomson D. D. (1995) *Marine mammals and noise*. San Diego: Academic Press, 1994.

Robinson, S. P., Lepper, P. A., Ablitt, J. (2007) The measurement of the underwater radiated noise from marine piling including characterisation of a "soft-start" period, *IEEE Oceans – Europe* 2006.

Robinson, S. P., Hayman, G. Lepper, P. A., Cucknell, A. C., Horswill, C., Duthie, N. (2009a) *Greater Gabbard offshore wind farm - Underwater noise monitoring during marine piling*. Gardline Environmental Report 7963 (Draft V.2) to Fluor Ltd July 2009.

Robinson, S. P., Lepper, P. A., Theobald, P. D., Ablitt, J., Hayman, G., Beamiss, G. A., Dible, S. (2009b) A methodology for the measurement of radiated noise from marine piling. *Proceedings of the 3rd Underwater Acoustic Measurement: Technology and Results Conference (UAM 2009)*.

Robinson, S. P., Theobald, P. D., Hayman, G., Wang, L-S., Lepper, P. A., Humphrey, V. and Mumford, S. (2011) *Measurement of noise arising from marine aggregate dredging operations*. MALSF (MEPF Ref no. 09/P108).

Robinson, S.P., Lepper, P.A. and Hazelwood, R. A. (2014) NPL Good Practice Guide No. 133, *Good Practice Guide for Underwater Noise Measurement*, ISSN: 1368-6550, 2014

Sand, O., Enger P. S., KaRLen H. E., Knudesen, F. R. (2001) Detection of infrasound in fish and behavioural responses to intense infrasound in juvenile salmonids and European silver eels: a mini review, *Am. Fish Soc. Symp.*, 26, pp. 183 - 193.

Sigray, P. and Andersson, M. H. (2011) Particle motion measured at an operational wind turbine in relation to hearing sensitivity in fish. *J. Acoust. Soc. Am.*, 130, pp. 200-206.

Smartwind (2013) *Hornsea offshore wind farm Project One, Environmental Statement Volume 4 – Introductory Annexes, Annex 4.3.2 Subsea noise technical report*, PINS Document Reference: 7.4.3.2, Report Number: UK04-050200-REP-0053, SMartwind, July 2013.

Southall, B. L., Bowles, A. E., Ellison, W. T., Finneran, J. J., Gentry, R. L., Greene Jr., C. R., Kastak, David, Ketten, D. R., Miller, J. H., Nachtigall, P. E., Richardson, W. J., Thomas, J. A.,

and Tyack, P. L. (2007) Marine Mammal Noise Exposure Criteria: Initial Scientific Recommendations, *Aquatic Mammals*, 33 (4), pp. 411-509.

Theobald, P. D., Lepper, P. A., Robinson, S. P., and Hazelwood, R. A. (2009) Cumulative noise exposure assessment for marine using Sound Exposure Level as a metric. *Proceedings of the 3rd International Conference & Exhibition on "Underwater Acoustic Measurements: Technologies & Results*", Napflion, Greece, June 2009, ISBN; 978-960-98883-4-9.

Theobald, P. D., Robinson, S. P., Lepper, P. A., Pangerc, T., Lloyd, N. (2010) *Underwater noise monitoring during marine piling*. Gardline Environmental Report 8503 to Fluor Ltd September 2010. Gardline Environmental Report 8503 to Fluor Ltd September 2010.

Thiele, R. (2002). *Propagation loss values for the North Sea*. Handout Fachgesprach: Offshore-Windmills-sound emissions and marine mammals. FTZ-Busum, 14.01.2002.

Thomsen, F., Lüdemann, K., Kafemann, R. and Piper, W. (2006) *Effects of offshore wind farm noise on marine mammals and fish, biola*. Hamburg, Germany on behalf of COWRIE Ltd.

Thorpe, W. H. (1967) Analytic description of the low frequency attenuation coefficient. *J. Acoust. Soc. Am.*, 42, pp. 270-270.

Tougaard, J. and Henriksen, O. D. (2009) Underwater noise form three types of offshore wind turbines: Estimation of impact zones for harbour porpoises and harbour seals. *J. Acoust. Soc. Am.*, 125, pp. 3766-3773.

Urick, R. J. (1983) *Principles of Underwater Sound*, Peninsula Publishing, New York.

Wahlberg, M. and Westerberg, H. (2005) Hearing in fish and their reactions to sounds from offshore wind farms. *Mar.Ecol. Prog. Ser.*, 288, pp. 295 - 309

Wang, L., Heaney, K., Pangerc, K., Theobald, P., Robinson, S, and Ainslie, M. (2014) Review of underwater acoustic propagation models, NPL Report AC 12.

Weston, D. (1976) Propagation in water with uniform sound velocity but variable-depth lossy bottom. *Journal of Sound and Vibration*, 47, pp. 473-483.

Yelverton, J. T., Richmond, D. R., Hicks, W., Saunders, K. and Fletcher, E. R. (1975) *The relationship between fish size and their response to underwater blast*. DNA 3677T, Lovelace Foundation for Medical Education and Research, Final Technical Report, June 1974.

9.7 Annex A – Introduction to Propagation Modelling

73. This annex introduces some basic underwater acoustic concepts which are in widespread use.

9.7.1 Metrics and Units

74. Two primary acoustic amplitude parameters have been widely used in the UK in relation to marine piling. These are peak-to-peak pressure (Nedwell et al. 2006; Nedwell et al. 2007), and Sound Exposure Level (SEL) (Southall et al. 2007). In addition, for some exposure criteria, the zero-to-peak or peak pressure level has been widely used (Southall et al. 2007).

75. The peak pressure refers to the pressure amplitude of the pulse where, often described as the peak positive pressure, and peak-to-peak pressure is the difference between the peak positive pressure and the peak negative pressure of the pulse. It is common to state these levels in decibels (dB) as a zero-to-peak pressure level (PPL) for peak pressure referenced to a zero-to-peak pressure of 1 μPa. The Sound Exposure Level is effectively a measure of the pulse energy content and is calculated from the integral of the squared sound pressure over the duration of the pulse (Madsen 2005; Ainslie 2011). It is also used to express the overall exposure (SEL dose), which in this case is done by summation of sound exposure levels of the entire piling event. The SEL can also be expressed in dB notation referenced to 1 μPa^2·s.

76. It should be noted that the metric used for continuous type sounds is different to those used for impulsive sounds like piling. For continuous noise such as vessel noise or operational turbine noise, the Sound Pressure Level (SPL) metric would normally be used which by convention describes the root mean square (RMS) level over a one second interval referenced to an RMS pressure of 1 μPa, and can also refer to the mean-square sound pressure level referenced to 1 μPa^2.

9.7.1.1 Zero-to-peak pressure level (PPL)

77. For a specific pulse or waveform, the peak pressure level, *PPL*, is defined as the zero-to-peak pressure of the pulse and can be expressed as the zero-to-peak pressure level (or peak pressure level, PPL) in units of dB re 1 μPa:

$$PPL \quad = \quad 20 \log \left[\frac{P_{zero-to-peak}}{P_0} \right]$$

where P_0 is the zero-to-peak reference pressure of 1 μPa.

9.7.1.2   Peak-to-peak acoustic pressure

78.   For a specific pulse or waveform, the peak-to-peak pressure, $P_{pk\text{-}pk}$, is calculated from the difference between the peak positive or maximum pressure p_{max} and the peak negative or minimum pressure p_{min}:

$$P_{pk-pk} \quad = \quad p_{\max} - p_{\min}$$

79.   Since the peak negative pressure has a negative value, the peak-to-peak pressure is equivalent to the sum of the magnitudes of the peak positive and peak negative pressures. The value is usually expressed as the peak-to-peak pressure level in dB re 1 µPa. This level is calculated from:

$$PL_{pk-pk} \quad = \quad 20 \log \left[\frac{P_{pk-pk}}{P_{0\,pk-pk}} \right]$$

where P_0 is the peak-to-peak reference pressure of 1 µPa.

80.   It should be noted that this metric has not been widely adopted outside of the UK or by the EC Marine Strategy Framework Directive (MSFD), Descriptor 11 for underwater noise (MSFD 2008). The MSFD has adopted the peak sound pressure level (in addition to the sound exposure level) defined as the zero-to-peak amplitude of the pulse (PPL). For consistency with the MSFD, all levels referenced from previous studies are either stated in their original form of peak, or converted where necessary from peak-to-peak to peak values by halving the value (subtracting 6dB), thereby assuming a symmetrical pulse shape.

81.   For this assessment, the approach of Southall et al. (2007) has been adopted such that the SPL term is always qualified to indicate the type of metric intended: for example, peak SPL, RMS SPL, etc. It should be noted that the peak SPL used by Southall et al. 2007 is equivalent to the zero-to-peak pressure level or PPL used here.

9.7.1.3   Sound Pressure Level (RMS SPL)

82.   The more common convention in underwater acoustics for expressing Sound Pressure Level (SPL) is for it to be expressed as a root mean square (RMS) value. The RMS value is a time-averaged pressure value, which allows the SPL to be related to the time-averaged acoustic power (the original use of the decibel notation is for expressing power ratios) (Carey 2006). This causes little problem for sinusoidal waveforms where there is a fixed relationship between the peak value of a sine wave and the RMS value. However, for pulse waveforms, there is no general relationship between the peak of the pulse and the RMS value (the RMS value for a pulse depends on the pulse length,

which depends on the pulse shape, the decay time, etc.) (Madsen 2005; Ainslie 2011). This can cause confusion and make comparisons between pulse type sounds and continuous type sounds meaningless even though they appear to be described using the same units.

83.   For this assessment, the root mean square of the sound pressure is used when considering continuous type noise sources(e.g. turbine operational noise) and can be expressed in units of dB re 1 μPa and is calculated from:

$$RMS\ SPL\ =\ 20\log\left[\frac{P_{RMS}}{P_0}\right]$$

where P_0 is the RMS reference pressure of 1 μPa.

9.7.1.4   Sound Exposure Level

84.   For a piling pulse, SEL is related to the sound energy in the pulse and is calculated by integrating the square of the pressure waveform over the duration of the pulse. The duration of the pulse is defined as the region of the waveform containing the central 90% of the energy of the pulse. The calculation is given by:

$$E_{90}\ =\ \int_{t_5}^{t_{95}} p^2(t)\,dt$$
.

85.   The value is then expressed in dB re 1 μPa^2·s and is calculated from:

$$SEL\ =\ 10\log\left[\frac{E_{90}}{E_0}\right]$$

where E_0 is the reference value of 1 μPa^2·s.

86.   Note that for a plane-wave in a free-field environment (an unbounded medium), the pulse pressure squared integral in μPa^2·s can be converted to units of energy flux density in joules per square metre (J·m^{-2}) by dividing the cumulative squared acoustic pressure by the specific acoustic impedance, Z, of the medium, the specific acoustic impedance being the product of the medium density and sound speed in the medium (ρc). When expressed in decibel notation, this means that 0dB re 1 J·m^{-2} is equivalent to 182dB re 1 μPa^2·s in water. Note also that the definition above uses the central 90% of the energy in the pulse (i.e., the pulse duration is defined as the time occupied by the central portion of the pulse) where 90% of the pulse energy resides. This is because it can be difficult to determine the exact start of the pulse when the

waveform contains noise. For the 100% value of SEL, it would be necessary to add 0.45dB to the 90% value.

87. The SEL for each impulsive noise event can also be aggregated by summation to calculate the total SEL (or SEL dose) for the entire piling sequence (Southall et al. 2007; Theobald et al. 2009). The concept of SEL dose is entirely analogous to the use in air acoustics to quantify the total noise dose for a subject receiver. The pulse duration is defined as the time occupied by the central portion of the pulse, where 90% of the pulse energy resides.

88. The calculation of the pulse duration and SEL are described graphically in Plate 9.15. Image A shows a typical pulse waveform, and image B shows a plot of the normalised energy in the pulse waveform against time. Indicated on the plot are the 5% and 95% energy levels and the t_5 and t_{95} times that define the pulse duration.
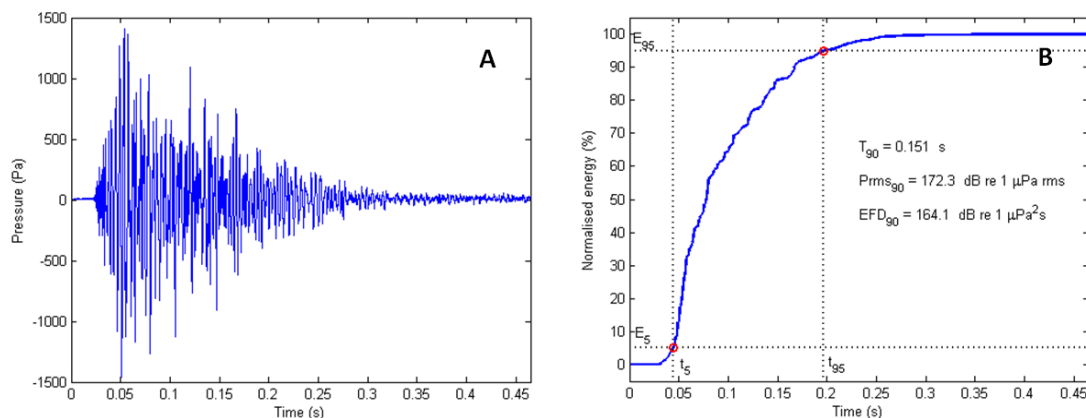

Plate 9.15. Example of pulse time waveform for analysis, and B: Calculation of SEL over pulse duration. Plots taken from NPL Good Practice Guide No. 133.

9.7.2 Sound Propagation Modelling

9.7.2.1 Environmental dependence

89. Perhaps even more so than for airborne sound, noise levels in the ocean produced by human activities are determined not only by the acoustic power output of the source, but equally importantly by the local sound transmission conditions (Urick 1983). A moderate level source transmitting over an efficient propagation path may produce the same received sound pressure level as a higher level source transmitting through a lossy propagation path (i.e. relatively higher TL). In deep water, variations in water properties strongly affect the sound propagation. In shallow water, effects due to the surface and bottom become more influential. Variations in bathymetry (depth) can have a significant effect on the transmission of the sound, and for piling noise significant proportions of the sound may be transmitted through the sea bed itself.

90. The sound speed profile may be divided into several layers. Just below the surface is what is sometimes called the surface layer where the speed is susceptible to daily changes due to heating, cooling and wind action. This is followed by a seasonal thermocline, a region characterised by a negative sound speed gradient due to the decrease in temperature with depth. Below the main thermocline and extending into the deep ocean is the deep isothermal layer, which is nearly constant in temperature at about 4 °C. In this layer, the sound speed increases with depth due to the increasing hydrostatic pressure. Between the thermocline and the isothermal layer is a sound speed minimum, toward which sound tends to be bent by the action of refraction. Some of the sound from a source placed in this channel can be trapped within the channel and travel great distances without appreciable losses due to surface or bottom reflections. Whilst spreading losses will still occur, they are reduced from spherical spreading and in certain cases may approximate to cylindrical spreading. The variation with salinity is less of an influence in deep water, but can have a strong influence where water layers of different salinity are mixing, for example at the estuaries of fresh-water rivers.

91. In shallow water around the UK coast, the sound speed is less likely to vary strongly with depth due to the shallow conditions, and the often rapid tidal flow which leads to a mixed isothermal water column.

92. The sound speed is such an important oceanographic parameter that it is routinely measured as a function of depth. This may be done using an instrument such as a velocimeter, which measures the time for a high frequency pulse to travel over a known path. Alternatively, a measurement is made of the conductivity (to derive salinity), temperature and depth using a CTD meter with the sound speed calculated form empirically-derived relationships.

9.7.2.2 Shallow water specific environmental dependence

93. One effect not always appreciated is that shallow water channels do not allow the propagation of low frequency signals due to the wave-guide effect of the channel (Urick 1983; Jensen et al. 2000). This effect means that there will be a lower cut-off frequency, below which sound waves will not propagate (instead the sound generated propagates into the sea bed).

94. For an idealised water channel consisting of a rigid bottom and a pressure-release surface, the cut-off corresponds to a quarter-wave resonance. However, for a realistic sea bed, a slightly more complicated formula depending on the ratio of sound speed in the bottom to that in the water can be used (Urick 1983). The result of plotting this formula is shown in Plate 9.16. The effect of the loss of sound from the water column due to shallow water is sometimes referred to as 'mode-stripping'.
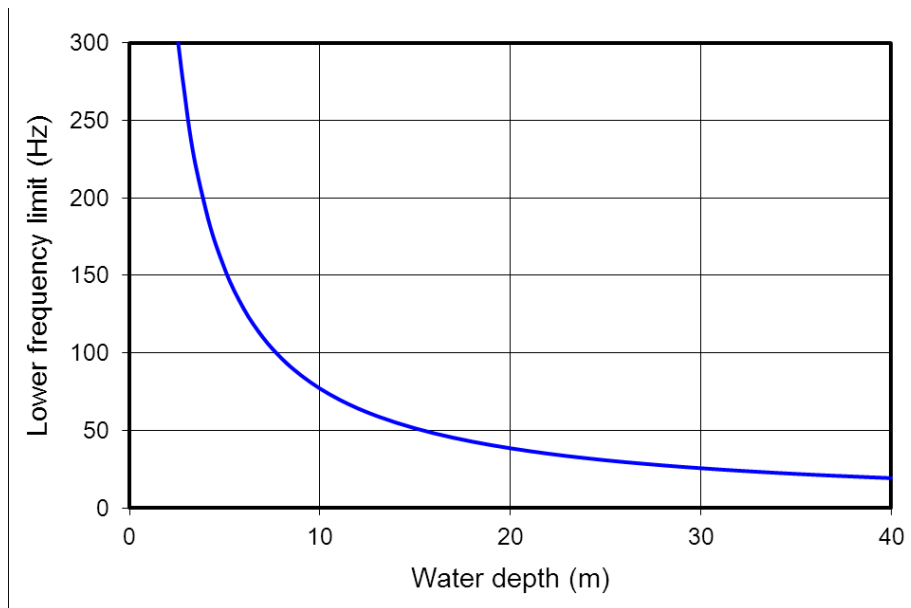
Plate 9.16. The lower cut-off frequency as a function of depth for a shallow water channel with for an example sea bed sound speed of 1702ms-1 (sand) and water sound speed of 1490ms-1.

95. It can be seen from Plate 9.16 that for a sandy sea bed and an approximate water depth of 20m, frequencies below around 40Hz would not be expected to propagate through the water. For piling, most of the energy in the resulting sound pulse falls between frequencies of around 100 and 400Hz.

9.7.2.3   Type of propagation model

96. The wave equation describing the propagation of an acoustic field is often difficult to solve in real-world situations. A good model describing the propagation of sound in the ocean should take into account:

- The interaction with the sea surface;

- The interaction with (and transmission through) the sea bed;

- The refraction of the sound due to the sound speed gradient;

- Absorption of the sound by the sea water and the sea bed;

- The geometrical spreading of the sound away from the source; and

- Relative source and receiver depth.

97. One common approach is to use a method of normal modes, often applied in cases where the sound speed is stratified (changes vertically with depth but not horizontally with range). The normal mode method is useful to calculate the field in shallow water where the water column acts as a waveguide for a limited number of propagating

modes. The theory can be expanded to account for different types of sea bed (assuming the properties are known), and variations in sound speed gradients. The problem of solving the wave equation for range dependent conditions such as sloping or irregular bottoms and range-varying sound speed profiles has been overcome by an approximation called the parabolic equation. Here, small incremental changes in range and depth are used to accommodate changes in propagation parameters without the occurrence of large errors. However, in deep water with large numbers of modes propagating, the method is computationally demanding (Lurton 2003; Richardson et al. 1995). The Parabolic Equation method provides a frequency domain solution for transmission loss and can provide distance and depth dependent transmission loss predictions. An alternative approach which can prove useful for broadband impulsive sounds is to use a time-domain approach such as a finite-difference method. This method has been used extensively in the geophysical surveying industry.

98. In water deep enough for propagation of ten or more modes, ray theory may be used. This requires that the sound speed changes slowly, with little change over a distance of one acoustic wavelength, making it best suited to the higher frequencies (and thus smaller wavelengths). The sound field is calculated by tracing ray paths, starting from the source, at uniformly spaced angular intervals. For each increment in range, the ray direction is determined from the ray equations and the local gradient of sound speed versus depth. This method is useful in deep water, where a small number of rays transmit most of the acoustic energy from source to receiver, where there is a direct path from source to receiver, and where only a limited number of surface and bottom reflections contribute. For shallow water, the large number of reflected paths makes the method somewhat impractical (Lurton 2003; Richardson et al. 1995).

99. In simple cases, acceptable accuracy may be obtained by use of relatively simple geometrical spreading models. Commonly used models include spherical spreading (in decibel notation, this corresponds to a reduction in received level with range, r, of "$20.\log(r)$"), or cylindrical spreading, (corresponding to a reduction in received level with range of "$10.\log(r)$"). In practice, the spreading may lie somewhere between these two geometries and be described by "$N.\log(r)$" where N typically has a value between 10 and 20. Such simple models do not include the effect of absorption in the medium. This may be included in a simplified manner by introducing a term which describes the reduction due to absorption with range (leading to a term of the type "$\alpha.r$" where α is the absorption in dB per meter). A composite model of this kind would then be used to calculate the received level (RL) from the source level (SL) by: $RL = SL - N.\log(r) - \alpha.r$ (Nedwell et al. 2007). This type of model can also be adapted to include frequency dependent attenuation (Thiele 2002; Thomsen et al. 2006).

9.7.2.4   Comparison of models

100.   Simple "lumped parameter" spreading models which incorporate simplified absorption, and conform to the general type "$RL = SL - N.\log(r) - \alpha.r$", have been used in previous UK studies which attempt to estimate the likely noise levels generated by windfarm construction (Nedwell et al. 2007). These models have the advantage that they do not require a large amount of input data (only values of N and α), are simple to compute for measured values of received level versus range, and may be set up to replicate the apparent transmission loss of the sound measured during piling operations at other windfarm sites. However, the limitations of these models should be considered carefully. Such a model does not account for transmission loss effects due to changes in bathymetry, and so cannot (for example) predict the extra reductions in level caused by sand banks and shallow coastal areas (for example due to the effect of mode stripping). In addition, such models do not include reverberation or consider the sound transmitted through the sediment, except in a highly simplistic way (e.g., by use of a composite value of α). Such a model is also frequency independent if it is applied to a time-domain parameter such as peak-to-peak sound pressure. This means it will depend only on range from the source. In practice, the transmission of sound in shallow water will show a strong dependence on frequency due to the modal nature of the propagation and the frequency-dependent absorption in the water and in the sediment. These phenomena will cause the time waveform to distort during propagation away from the source, typically causing a dilation of the acoustic pulse (an increase in pulse duration) and a reduction in high frequency content.

101.   For the very shallow water environments, the normal mode and Parabolic Equation approach outlined above has the potential to provide good accuracy. This method can be made to incorporate the effects of variable bathymetry, sound speed profiles and frequency dependent absorption. However, such models do require a large amount of input data to describe the bathymetry, sound speed profiles, and sediment properties in the local area. Such information may not always be available, and any model is only as accurate as its input data. In addition, to describe the propagation of short broadband pulses, typically this type of model would be run at a number of discrete frequencies in order to predict the transmission loss at all the frequencies present in the pulse, and this requires greater computational power (and time).

102.   It should also be noted that the accuracy of any model depends on accurate representation of the source. The source in the case of marine piling is very complex, with noise being radiated from the surface of the pile itself, and with noise also being launched directly into the sea-bed by the impact of the pile through the sediment. Currently, a perfect model does not exist for such a complex distributed source, and

representations of the source in terms of simplified idealised sources such as point sources and line sources will inevitably limit the accuracy of predictions. This is particularly true for the acoustic field close to the pile (in the near-field), and possibly for greater ranges where sound propagating through the sea-bed re-enters the water column.

9.7.2.5 Choice of model

103. A propagation model must be adopted in order to make any attempt to estimate the acoustic field at ranges other than those where measurements have been made. For example, to estimate the acoustic field within a few hundred metres of the source from measurements made at greater ranges. Similarly, if the source is to be described in terms of simplified concepts such as source level (useful, for example, if there is a desire to make comparisons with other sources), a propagation loss model is needed in order to estimate the transmission loss required to derive the source level. For the work described here, the model adopted is the Energy flux model described by Weston (Weston 1976). This propagates the sound energy in the water column, and takes full account of geometric spreading, interaction with boundaries, modal propagation in shallow-water, frequency-dependent absorption in the water and sea bed, and scattering from the sea-surface (caused by wave agitation). The implementation of this model has been has benchmarked by NPL against several other standard models such as methods based on normal modes such as Kraken (c 1991) and CSNAP (Ferla et al. 1996), as well as the RAM parabolic equation solution (Collins 1993), and the OASES wave-number integration code (Goh and Schmidt 1996). The Weston model decomposes the acoustic field into one-third octave band levels and propagates each frequency band independently, recombining the frequency bands at a new range to calculate the broadband levels. A full review of the models described here and benchmarking of these models has been carried out by Wang et al. (2014), which also provides guidance on the choice of models for different environments.

9.8 Annex B – Model Validation with Windfarm Measurement Data

104. As part of the environmental impact assessment for East Anglia ONE, a benchmarking exercise was completed to compare the predicted received level outputs, obtained with the NPL implementation of the Weston energy flux model (see Section 9.3 for details), with those measured for foundation B10 at the Belwind Phase 1 windfarm, for which the measurements were reported in Degraer et al. (2010). This location was modelled using the Weston energy flux model and the results are shown for comparison in Table 9.8 below at the ranges for which measurements were reported for Belwind Phase I. The validation modelling was undertaken assuming a hammer energy of 1000kJ (slightly higher than reported) for ranges less than 14,150m, and 710kJ for the measurement reported at a range of 14,150m. Ranges less than 2,580m were not modelled as the necessary level of bathymetric data was not available. The predicted levels are slightly higher than the measured values, which is expected, as they were modelled for the highest astronomical tide conditions conducive to better underwater sound propagation in this instance. It is unknown what the tidal state during the time of measurements was, but it is expected that this may have varied during the course of the measurements. There is also some variation expected as the predicated results obtained through propagation modelling assume a straight easterly transect. The actual measurement transect was initially to the east and then deviated to the southeast further out.

Table 9.8. Benchmarking results of Weston Energy Flux model against measurements for Belwind Phase I reported in Degraer et al. (2010).

Measurement Range	Measured peak SPL (dB re 1 µPa)	Modelled peak SPL (dB re 1 µPa)
2580 m	174	178
4000 m	168	174
5500 m	169	172
7250 m	165	169
14150 m	160	161

105. A further model validation example of the implementation of the Weston energy flux model, used in this assessment, is provided in the Environmental Statement for the Hornsea Project One offshore windfarm, where a benchmarking exercise was carried out against measured data obtained during the installation of the meteorological mast in the Hornsea Zone (Smartwind 2013).

9.9 Annex C – Modelled Source Locations

Table 9.9. Summary of source (foundation) positions used to estimate potential impact ranges.

Location ID	Latitude (N) Dec. degrees	Longitude (E) Dec. degrees
1	52.7716	3.0377
2	52.5055	2.8092
3	52.5253	2.7593
4	52.7529	2.7594
5	52.7594	2.8555
6	52.7653	2.9422
7	52.5849	2.7593
8	52.6389	2.7593
9	52.6940	2.7594
10	52.5656	2.8605
11	52.6370	2.9217
12	52.7047	2.9799
13	52.7164	2.8269
14	52.7294	2.9122
15	52.7381	2.9794
16	52.6753	2.7955
17	52.6674	2.8799
18	52.6115	2.7943
19	52.6141	2.8755
20	52.5382	2.8075

9.10 Annex D – Piling sequence used in illustrative SEL dose modelling

Table 9.10. Example piling sequence

Hammer blow energy (kJ)	Duration (minutes)	Blows Per Minute	Number of strikes
1,400	20	30	600
2,000	30	30	900
2,300	30	30	900
3,000	30	30	900
3,500	120	30	3600

Appendix 9.1 Ends Here